*Journal of Experimental Botany*, Vol. 72, No. 7 pp. 2769–2789, 2021
doi:10.1093/jxb/erab031 Advance Access Publication 22 January 2021

RESEARCH PAPER

# High affinity promoter binding of STOP1 is essential for early expression of novel aluminum-induced resistance genes *GDH1* and *GDH2* in Arabidopsis

**Mutsutomo Tokizawa[1,2], Takuo Enomoto[1], Hiroki Ito[1], Liujie Wu[1,*], Yuriko Kobayashi[1], Javier Mora-Macías[2], Dagoberto Armenta-Medina[3,4], Satoshi Iuchi[5], Masatomo Kobayashi[5], Mika Nomoto[6], Yasuomi Tada[6], Miki Fujita[7], Kazuo Shinozaki[7], Yoshiharu Y. Yamamoto[1,7], Leon V. Kochian[2,†] and Hiroyuki Koyama[1,†]**

[1] Applied Biological Sciences, Gifu University, Gifu 501–1193, Japan
[2] Global Institute for Food Security, University of Saskatchewan, Saskatoon S7N 4J8, Canada
[3] CONACyT Consejo Nacional de Ciencia y Tecnología, Dirección de Cátedras, Insurgentes Sur 1582, Crédito Constructor, 03940 Ciudad de México, México
[4] INFOTEC Centro de Investigación e Innovación en Tecnologías de la Informacion y Comunicación, Circuito Tecnopolo Sur No 112, Fracc. Tecnopolo Pocitos II, 20313 Aguascalientes, México
[5] RIKEN Bioresource Research Center, Ibaraki 305-0074, Japan
[6] Center for Gene Research, Nagoya University, Nagoya 464–8602, Japan
[7] RIKEN Center for Sustainable Resource Science, Yokohama 230-0045, Japan

[†] Correspondence: leon.kochian@gifs.ca or koyama@gifu-u.ac.jp
* Present address: School of environment and life science, Nanning Normal University, Nanning 530001, China

Received 19 January 2021; Editorial decision 7 January 2021; Accepted 20 January 2021

Editor: Richard Napier, University of Warwick, UK

## Abstract

**Malate efflux from roots, which is regulated by the transcription factor STOP1 (SENSITIVE-TO-PROTON-RHIZOTOXICITY1) and mediates aluminum-induced expression of *ALUMINUM-ACTIVATED-MALATE-TRANSPORTER1* (*AtALMT1*), is critical for aluminum resistance in *Arabidopsis thaliana*. Several studies showed that *AtALMT1* expression in roots is rapidly observed in response to aluminum; this early induction is an important mechanism to immediately protect roots from aluminum toxicity. Identifying the molecular mechanisms that underlie rapid aluminum resistance responses should lead to a better understanding of plant aluminum sensing and signal transduction mechanisms. In this study, we observed that GFP-tagged STOP1 proteins accumulated in the nucleus soon after aluminum treatment. The rapid aluminum-induced STOP1-nuclear localization and *AtALMT1* induction were detected in the presence of a protein synthesis inhibitor, suggesting that post-translational regulation is involved in these events. STOP1 also regulated rapid aluminum-induced expression for other genes that carry a functional/high-affinity STOP1-binding site in their promoter, including *STOP2*, *GLUTAMATE-DEHYDROGENASE1* and *2* (*GDH1* and *2*). However STOP1 did not regulate Al resistance genes which have no functional STOP1-binding site such as *ALUMINUM-SENSITIVE3*, suggesting that the binding of STOP1 in the promoter is essential for early induction. Finally, we report that *GDH1* and *2* which are targets of STOP1, are novel aluminum-resistance genes in Arabidopsis.**

**Keywords:** Acid soil, aluminum tolerance, *ALUMINUM-ACTIVATED MALATE TRANSPORTER 1 (ALMT1)*, *Arabidopsis thaliana*, *GLUTAMATE DEHYDROGENASE (GDH)*, *In silico* promoter *cis*-elements prediction, post-translational regulation, promoter analysis, *SENSITIVE TO PROTON RHIZOTOXICITY1 (STOP1)*, transcriptional regulation.

## Introduction

Rhizotoxicity of aluminum (Al) is one of the most serious environmental factors that limit food production in the world. Al appears in acid soils [pH ($H_2O$)<5.5] that cover about 40% of the world's arable lands including emerging countries in tropical and sub-tropical regions (von Uexküll and Mutert, 1995). The root exudation of organic acids (e.g. malate and citrate) into the rhizosphere is a conserved Al stress adaptation mechanism among a wide range of terrestrial plant species (Kochian *et al.*, 2004; 2015; Barros *et al.*, 2020). ALUMINUM-ACTIVATED-MALATE-TRANSPORTER1 (AtALMT1) was originally identified as a critical Arabidopsis gene for Al resistance, which is an important trait for crop plants grown on acidic soils (Sasaki *et al.*, 2004; Hoekenga *et al.*, 2006). This gene also has regulatory roles related to other important agronomic traits. For example, malate secreted from roots recruits beneficial rhizobacteria, which can enhance plant immune responses (Rudrappa *et al.*, 2008; Lakshmanan *et al.*, 2012; Kobayashi *et al.*, 2013b), and can modify root architecture under phosphorus (P)-deficient conditions (Balzergue *et al.*, 2017; Mora-Macías *et al.*, 2017). Additionally, *AtALMT1* expression is activated by a number of different stimuli and signals, including Al, P-deficiency, microbe-associated molecular patterns (e.g. FLG22 peptides), $H_2O_2$, indole-3-acetic acid, and abscisic acid (Lakshmanan *et al.*, 2012; Kobayashi *et al.*, 2013a; Balzergue *et al.*, 2017). Studies of molecular mechanisms underlying transcriptional regulation of *AtALMT1* are necessary to better understand how *AtALMT1* regulates such a range pleiotropic responses.

Previous time-course and dose-response analyses of root *AtALMT1* expression revealed that Al exposure rapidly induces *AtALMT1* expression in the root tip within one hour, and the expression continues to increase in response to long-term Al exposure (Kobayashi *et al.*, 2007; Liu *et al.*, 2009; Ding *et al.*, 2013). Analysis of the *AtALMT1* promoter led to the identification of several transcription factors and *cis*-acting elements that regulate different phases of *AtALMT1* expression (Tokizawa *et al.*, 2015). For example, the Al-inducible expression of *CALMODULIN-BINDING-TRANSCRIPTION-ACTIVATOR2* (*CAMTA2*) activates the late phase of *AtALMT1* expression (Tokizawa *et al.*, 2015). In addition, the transcription factor SENSITIVE-TO-PROTON-RHIZOTOXICITY1 (STOP1) binds directly to the *AtALMT1* promoter, which contains a GGNVS consensus sequence that serves as the binding site of the rice STOP1 ortholog (i.e. AL-RESISTANCE-TRANSCRIPTION-FACTOR 1; ART1; Yamaji *et al.*, 2009; Tsutsui *et al.*, 2011), and is essential for *AtALMT1* expression in both the early and late phases of Al exposure (Iuchi *et al.*, 2007; Tokizawa *et al.*, 2015). Since *STOP1* expression is not responsive to Al (Iuchi *et al.*, 2007; Kobayashi *et al.*, 2014), early Al-induced *AtALMT1* expression presumably is regulated by mechanisms other than transcriptional regulation, such as post-translational regulation of STOP1. In fact, an F-box protein, REGULATION-OF-ATALMT1-EXPRESSION 1 (RAE1), HYPERRECOMBINATION-PROTEIN 1 (HPR1), and EARLY-IN-SHORT-DAYS 4 (ESD4) were reported to modulate the expression of STOP1-regulated genes by post-transcriptional and post-translational regulation of STOP1 (Zhang *et al.*, 2019; Guo *et al.*, 2020; Fang *et al.*, 2020). RAE1, HPR1, and ESD4 are involved in STOP1 degradation through the ubiquitin-26S proteasome pathway, STOP1 mRNA export from nucleus, and SUMOylation of STOP1, respectively, thus regulating STOP1 protein abundance in the roots. In addition, a recent study confirmed that green fluorescent protein (GFP)-tagged STOP1 accumulates in the nucleus in response to P deficiency, resulting in the activation of *AtALMT1* transcription (Balzergue *et al.*, 2017). Additionally, STOP1 nuclear accumulation is also stimulated by Al under low P conditions, and this accumulation was observed soon after +Al/–P treatment (1 h; Godon *et al.*, 2019). Considered together, these studies suggest that post-translational STOP1 nuclear accumulation may be the limiting factor for the induction of STOP1-regulated genes such as *AtALMT1*.

The STOP1 zinc finger transcription factor was originally isolated from an *A. thaliana* mutant that was hypersensitive to proton rhizotoxicity (i.e. plant growth was inhibited in low-pH medium; Iuchi *et al.*, 2007). Subsequent systems biology-based analyses indicated that STOP1 regulates a number of *A. thaliana* genes that confer resistance to Al stress, including *AtALMT1*, *AtMATE* (*MULTIDRUG-AND-TOXIC-COMPOUND-EXTRUSION*, which encodes a root citrate efflux transporter), and *ALS3* (*ALUMINUM-SENSITIVE 3;* Larsen *et al.*, 2005; Gabrielson *et al.*, 2006; Liu *et al.*, 2009; Sawaki *et al.*, 2009; Ohyama *et al.*, 2013). Additionally, the expression of a unique Arabidopsis *STOP1* homolog, *STOP2*, is regulated by STOP1 (Kobayashi *et al.*, 2014). However, whether these genes are directly or indirectly regulated by STOP1 is still not known. Moreover, during the initial responses to Al exposure, STOP1 may be activated by Al and bind to the *AtALMT1* promoter to up-regulate its expression. If this model is correct, we theoretically should be able to detect the STOP1-regulated transcriptional activation of several other genes.

In this study, we investigated the early events related to Al-induced activation of STOP1-dependent expression of

*AtALMT1*, using cellular and molecular biology approaches. Several studies have reported that toxic Al ions very rapidly (within 5–30 min after treatment) inhibit root growth (Jones and Kochian, 1995; Krtková *et al.*, 2012; Kopittke *et al.*, 2015). Therefore, early *AtALMT1* induction is an important event to rapidly protect the roots from Al toxicity. Additionally, identification of the molecular mechanisms underlying the early Al response triggering *AtALMT1* transcription should lead to a better understanding of plant Al sensing/transduction mechanisms. In this study, we observed nuclear accumulation of STOP1 soon after Al treatment. In addition, a combination of *cis*-element prediction, *in vitro/vivo* protein-DNA binding assays, as well as *in planta* promoter::*GUS* expression revealed that early Al-inducible expression occurred in other previously unidentified genes, including *STOP2, GLUTAMATE-DEHYDROGENASE1* and *2 (GDH1* and *2)*, which contain a high affinity STOP1-binding site in their promoters. Finally, we discovered that the *GDH* genes are Arabidopsis novel Al resistance genes, that confer resistance via internal Al tolerance mechanisms. This finding has expanded our understanding of physiological targets of Al toxicity in plants, and uncovers additional characteristics of STOP1 in transcriptional regulation of Al tolerance genes in Arabidopsis.

## Materials and methods

### Plant materials

*Arabidopsis thaliana* (accession Col-0) was obtained from the RIKEN Bioresource Research Center (Tsukuba, Japan). The *STOP1*-KO (SALK_114108), and the series of *gdh* mutants [the *gdh1* (SALK_042736), *gdh2* (SALK_102711), and *gdh1/2* double mutant] were identical to those used by Sawaki *et al.* (2009) and Miyashita and Good (2008). Transgenic *A. thaliana* lines expressing the *GUS* gene under the control of the *AtALMT1*, *STOP2*, *GDH2*, *AtMATE*, or *ALS3* promoters, or the fusion construct encoding STOP1-GFP were generated using a floral dip method involving *Agrobacterium tumefaciens* strain GV3101 cells. The *STOP1-GFP* construct (for a GFP tag at the C-terminal of STOP1) was fused with the *STOP1* promoter (−2848 bp from the ATG start codon) and the downstream region of *STOP1* (+626 from the stop codon). Additionally, *GUS* was placed under the control of the promoters for the following genes with or without a mutation in the STOP1-binding sequence: *ALS3* (1000, 750, 500, 338, 238, 138, and 87 bp from the ATG start codon), *AtMATE* and *GDH2* [1000 bp from the transcription start site (TSS)], *STOP2* (1500 bp from the TSS), and *AtALMT1* (1100 bp from the TSS). Mutation in the STOP1 binding sequence in *AtMATE* (– 100 to –93 bp from the TSS, GGGGGCAC to AAAAAAAA), *STOP2* (–938 to –931 bp from the TSS, TCCGGGGG to AAAAAAAA), *GDH2* promoter (–592 to –585 bp from the TSS, CCGTCCCC to AAAAAAAA) was introduced by PCR using specific primers (Supplementary Table S1). Details regarding the TSSs were obtained from a published study (Tokizawa *et al.*, 2017). All promoter::gene constructs were generated by an overlap extension PCR using gene-specific primers (Supplementary Table S1) and the PrimeSTAR MAX high-fidelity Taq polymerase (Takara Bio, Ohtsu, Japan). The resulting constructs were then ligated into the pBE2113 vector (Mitsuhara *et al.*, 1996) carrying a kanamycin resistance gene. The *AtALMT1* promoter::GUS with or without a mutation in the STOP1-binding site (i.e., CIS-D region in *AtALMT1* promoter, see Tokizawa *et al.*, 2015) were identical to those reported in a previous study, and the mutation to the CIS-D sequence severely inactivated *AtALMT1* promoter activity and the associated Al-induced response (Tokizawa *et al.*, 2015).

### Conditions for aluminum and/or chemical treatments and root growth test

*Arabidopsis thaliana* seedlings were grown in the MGRL hydroponic culture solution (pH 5.5; Fujiwara *et al.*, 1992) modified as previously described (Kobayashi *et al.*, 2007), and five and ten day-old seedlings were used to analyse GFP fluorescence and transcript abundance, respectively. The pre-grown seedlings were transferred to 10 μM $AlCl_3$ stress treatment solutions with or without 10 μM cycloheximide (CHX) (Wako, Osaka, Japan). The CHX treatment was completed after a 30 min pre-incubation in the MGRL medium (pH 5.5). Unless otherwise indicated, all chemicals were purchased from Nacalai Tesque, Tokyo, Japan.

The root growth assays were conducted as previously described (Kobayashi *et al.*, 2007). Briefly, we measured the root lengths of five day-old seedlings grown in control or toxic Al (4 μM $AlCl_3$) solutions. Root lengths were measured for 15 seedlings using the image processing program, ImageJ. The potential Al tolerance of each genotype was evaluated by using the five longest roots to calculate mean values and standard errors of relative root lengths [RRL; root length in Al solution/root length in control solution].

### Analysis by confocal microscopy

Images of the roots of transgenic plants producing GFP were obtained with an LSM-710 laser-scanning confocal microscope (Carl Zeiss, Tokyo, Japan). Fluorescence in the roots of five day-old transgenic seedlings producing STOP1-GFP proteins was observed according to the supplier's recommended protocols. GFP was excited at 488 nm with an argon laser, and fluorescence (493–536 nm) was observed. Meanwhile, mCherry was excited at 543 nm with a He/Ne laser, and the emission (587–688 nm) was observed. Images were analysed using ZEN software (Carl Zeiss).

### Prediction of cis-acting elements in the promoters of STOP1-regulated genes

Putative *cis*-acting elements in the STOP1-regulated genes [i.e. suppressed Al-inducible expression in the *stop1* mutant (Sawaki *et al.*, 2009); Supplementary Table S2] were predicted by analysing the over-represented octamer units (Yamamoto *et al.*, 2011). Comparisons with the octamer units of genome-wide promoters identified over-represented octamer units in the promoters (0 to −1000 bp from the TSS]) of 249 *stop1*-suppressed genes [fold-change compared with wild-type >1/2.5; the microarray data and selected genes were previously reported by Sawaki *et al.* (2009) and Tokizawa *et al.* (2015), respectively]. The RAR (i.e. relative appearance ratio of octamer units in STOP1-regulated genes to octamer units in genome-wide promoters) and statistical significance (Fisher's exact test) were calculated for each octamer unit. Putative STOP1-binding sites in the promoters of STOP1-regulated genes were predicted based on a RAR >5 ($P$<0.05) and the presence of the GGNVS fragment (i.e. putative consensus sequence of the rice STOP1-like binding site, Tsutsui *et al.*, 2011; Supplementary Table S3). Additionally, putative Al-responsive *cis*-acting elements in the *ALS3* promoter were predicted using 266 Al-inducible genes (fold-change compared with the control <3; Sawaki *et al.*, 2009; Tokizawa *et al.*, 2015). Two putative elements (CIS-Y and CIS-Z) were predicted based on a RAR >3 ($P$<0.05). The predicted STOP1-binding sites were characterized by an *in vitro* STOP1-binding assay followed by an *in planta* promoter GUS assay.

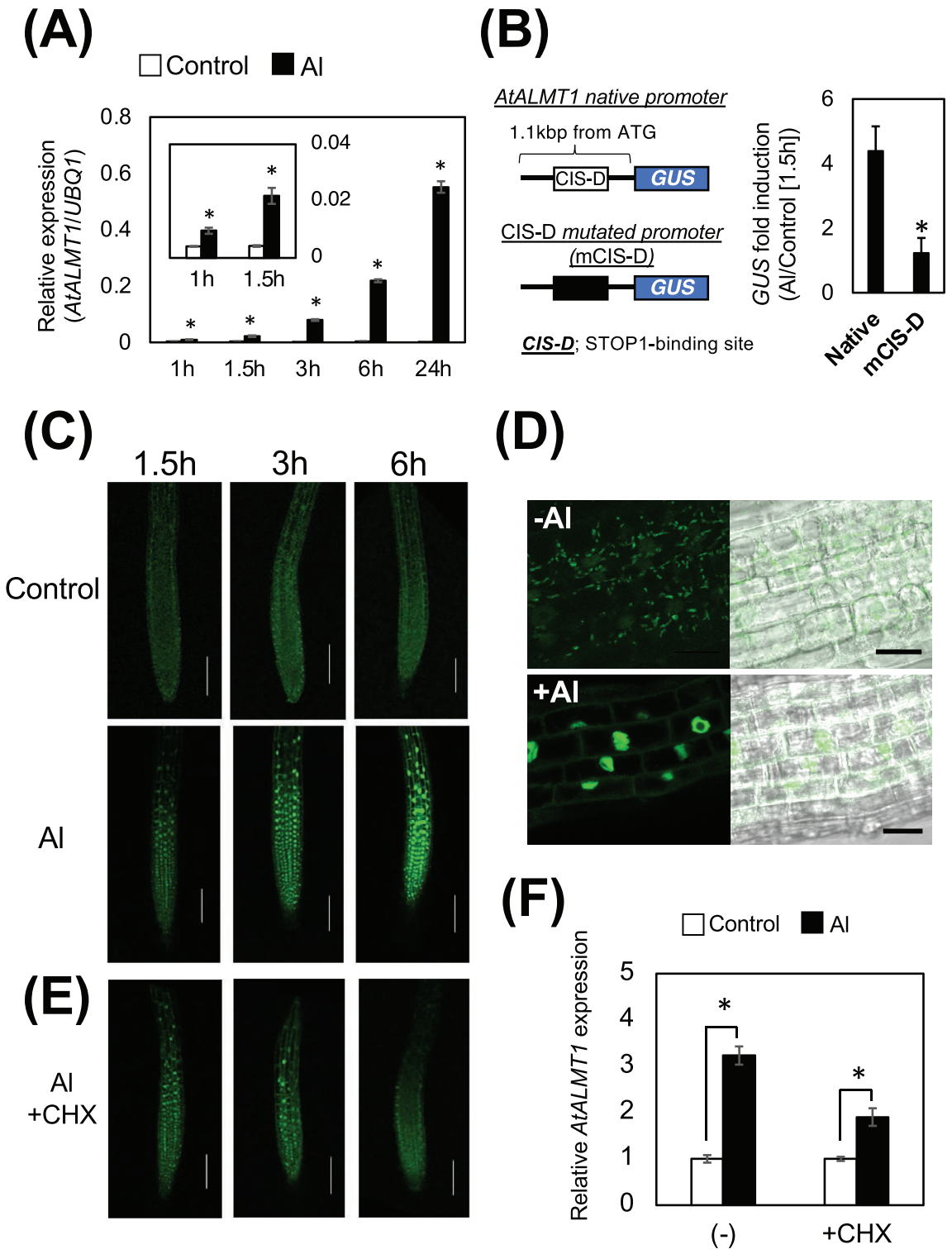


**Fig. 1.** *AtALMT1* expression and localization of STOP1-GFP in the nucleus during early responses to Al. The roots of hydroponically grown *A. thaliana* Col-0 (A, F), transgenic Col-0 expressing *GUS* under the control of the native *AtALMT1* promoter (0 to −1100 bp from the ATG start codon; Native) or the *AtALMT1* promoter mutated (mCIS-D) at the STOP1-binding site (B), and transgenic Col-0 carrying the *STOP1 promoter::STOP1-GFP* (C, D, E) were treated with 10 μM $AlCl_3$ (pH 5.5) or control solution (no $AlCl_3$, pH 5.5). (A) Time course of Col-0 *AtALMT1* expression in the presence (black bar) or absence (white bar) of 10 μM $AlCl_3$. (B) Short-term (1.5 h) Al-responsive *GUS* expression in transgenic *A. thaliana* expressing *GUS* under the control of the mCIS-D or native promoter [see Tokizawa *et al.* (2015)]. (C) Fluorescence of GFP-tagged STOP1 in Arabidopsis roots following control and Al

Several *cis*-acting elements of the *ALS3* promoter were also characterized in *in vivo* GUS expression assays using transgenic *A. thaliana* plants with or without mutations at predicted sites.

### *In vitro STOP1/dsDNA interaction assay*

FLAG (DYKDDDDK)-tagged STOP1 proteins were synthesized in an *in vitro* transcription/translation system following the method described previously (Nomoto and Tada, 2018). Biotinylated and unlabeled oligo-DNAs were obtained from the supplier and used for dsDNA synthesis (i.e. biotinylated and control). Sequence details for all probes used in this study are provided in Supplementary Table S4. The *in vitro* assays examining the binding between STOP1 and the dsDNA probes were completed using the AlphaScreen FLAG (M2) Detection Kit (PerkinElmer, Tokyo, Japan) according to our previous study (Tokizawa *et al.*, 2015). Briefly, the FLAG-tagged STOP1 protein and biotinylated dsDNA were treated with anti-FLAG antibody-coated donor beads and streptavidin-coated acceptor beads. The chemiluminescence generated by the conjugation of the acceptor and donor beads (i.e. AlphaScreen signal) was quantified using the Enspire Multimode plate reader (PerkinElmer). The AlphaScreen assay was conducted according to the protocol recommended by the supplier, while the competitive assay was completed in the presence of a ten-fold higher concentration of competitor.

### *Extraction of total RNA and the subsequent quantitative real-time PCR*

The extraction of total RNA from the roots, reverse transcription, and quantitative real-time (qRT)–PCR were carried out as previously described (Tokizawa *et al.*, 2015). Briefly, total RNA was extracted from the roots using Sepasol-RNA I Super G (Nacalai Tesque INC., Kyoto, Japan) and then reverse transcribed with ReverTra Ace (Toyobo, Osaka, Japan). All qRT–PCRs were conducted using standard curve methods with the THUNDERBIRD SYBR qPCR Mix (Toyobo). Details regarding the gene-specific primers are provided in Supplementary Table S1. The presence of contaminating genomic DNA during the qRT-PCR assay was checked using templates that had not undergone a reverse transcription step. The *UBQ1* gene (At3g52590) was used as the internal standard for expression analysis, and we validated that *UBQ1* expression was stable under our experimental conditions (Supplementary Fig. S1A). In addition, using gene expression database GENEVESTIGATOR (Hruz *et al.*, 2008), we confirmed that *UBQ1* is stably expressed in roots and any developmental stage, which is comparable to other well-known internal control genes (Supplementary Fig. S1B, C). A total of 803 public Affymetrix ATH1 genome array data of roots, which were obtained from GENEVESTIGATOR, were used for the evaluation of stable *UBQ1* expression in roots.

### *Chromatin immunoprecipitation (ChIP)*

ChIP analysis was performed following the method described previously with few modifications (Gendrel *et al.*, 2005; Ogita *et al.*, 2018). The 10 day-old seedlings of Col-0 and transgenic Arabidopsis that expressed *STOP1* promoter::STOP1-GFP were treated with $AlCl_3$ for 1.5 h and 6 h, or without Al. Roots (about 120 mg) were collected, and the cross-linking reaction was conducted using 1% formaldehyde (Sigma-Aldrich, USA) under vacuum. The chromatin was extracted from the fixed root samples, and subjected to fragmentation reaction using a sonic dismembrator M120 (Fisher science, USA; 50% amplitude, and 10 s "ON" /2 min "OFF" for 23 cycles). To immunoprecipitate STOP-GFP, an anti-GFP polyclonal antibody (A6455, Invitrogen, USA) and Dynabeads™ Protein G (Invitrogen, USA) were used. To qualify immunoprecipitated DNA, quantitative real-time PCR assay was conducted, and the enrichment of PCR products from the immunoprecipitated DNA was normalized by corresponding input DNA sample. Primers used for the ChIP-qPCR assay are shown in Supplementary Table S1. The primers for *Mutator-like transposon* (*Mu-like*) were used as negative control (Sauret-Güeto *et al.*, 2013). Two independent assays were performed, and similar results were obtained.

## Results

### *Early Al-induced* AtALMT1 *expression and STOP1 localization in the nucleus*

When 10 day-old seedlings grown in control medium were exposed to a solution containing 10 μM $AlCl_3$, *AtALMT1* expression was activated within 1.5 h (Fig. 1A). To determine whether this activation required the binding of STOP1 to the *AtALMT1* promoter, an *in planta* promoter assay was conducted with transgenic *A. thaliana* plants in which *GUS* expression was regulated by the *AtALMT1* promoter (1100 bp region from the ATG start codon) with or without a mutation in the STOP1-binding domain. The mutation was introduced into the consensus GGNVS STOP1 binding sequence (designated as the CIS-D region by Tokizawa *et al.*, 2015). The mutated promoter is hereafter called mCIS-D. *GUS* expression under the mCIS-D promoter was significantly lower ($P<0.05$, Student's *t*-test) than *GUS* expression driven by control of the native promoter after 1.5 h of Al exposure (Fig. 1B). This suggested that the early activation of *AtALMT1* expression involves a process induced by the interaction between STOP1 and the CIS-D region of the promoter.

To characterize the mechanism responsible for the STOP1-mediated activation of *AtALMT1* transcription, we prepared *STOP1 promoter::*STOP1-GFP transgenic plants. The STOP1-GFP fluorescence pattern differed between control and Al treatments (Fig. 1C). Under control conditions, STOP1-GFP fluorescence was localized as punctate spots, which contrasted with general cytosolic localization for GFP fluorescence (Fig. 1D; Supplementary Fig. S2). However, in response to Al treatment, STOP1-GFP was localized to the nucleus (Fig. 1D). This change in localization was induced within 1.5 h of Al treatment

treatments for 1.5, 3, and 6 h. Bar =100 μm. (D) Magnified image of STOP1-GFP fluorescence in Arabidopsis roots at 6 h after control (no Al) and Al treatments. (E) Fluorescence of STOP1-GFP in Arabidopsis roots after 10 μM $AlCl_3$ and $AlCl_3$ plus 10 μM cycloheximide (CHX) treatments. The CHX treatment included a 30 min pre-incubation in control medium followed by a co-incubation with Al and CHX. Bar =100 μm. (F) Effect of CHX on the early Al-inducible expression of *AtALMT1*, evaluated after a 1.5-h incubation in medium containing $AlCl_3$ (0 or 10 μM) and CHX (0 or 10 μM). *UBQ1* expression was used to normalize *AtALMT1* (A, F) and *GUS* (B) expression. The control *AtALMT1* expression was set as 1 (F). In the transcript analyses (A, B, F), asterisks indicate a significant difference (*$P$ <0.05; Student's *t*-test). Data are presented as the mean ±SD ($n$=3). All experiments were repeated at least three times, with similar results.

(Fig. 1C; Supplementary Video S1). These results imply that the localization of STOP1 to the nucleus is associated with the early Al-mediated response of STOP1, which may contribute to the activation of *AtALMT1* expression.

The Al-induced accumulation of STOP1-GFP in the nucleus was repressed during a 6 h Al exposure in the presence of a protein synthesis inhibitor cycloheximide (CHX; 30 min pre-incubation and then an Al co-treatment, Fig. 1E). However, in the early Al-induced phase (1.5 h of Al exposure), the accumulation of STOP1-GFP in the nucleus and up-regulated *AtALMT1* expression were still observed in the presence of CHX (Fig. 1E, F). Thus, the localization of STOP1 in the nucleus, which is post-translationally regulated, appears to be involved in early Al-induced *AtALMT1* expression, which is consistent with STOP1 as a transcription factor, activating *AtALMT1* expression.

### *Identification of several genes carrying a STOP1-binding site in their promoter*

Al-induced *AtALMT1* expression requires the binding of STOP1 to a functional binding site in the promoter (Fig. 1B) and also localization of STOP1 to the nucleus soon after Al exposure (Fig. 1C). Accordingly, we speculated that other genes with functional STOP1-binding sites in their promoters might exhibit similar transcriptional responses. To investigate instances of STOP1-dependent regulation in other genes, the promoters of other genes containing functional STOP1-binding sites were first identified by promoter bioinformatics analyses and then *in vitro* binding and *in planta* promoter assays. These were similar to approaches we previously used to detect the STOP1-binding site in the *AtALMT1* promoter (Tokizawa *et al.*, 2015). The STOP1-binding motif was predicted to be contained in the promoters of 15 genes whose expression was then found to be suppressed by a *stop1* mutation under Al stress conditions (fold-change <1/3; Supplementary Table S2). A schematic explaining these analyses is presented in Fig. 2A. The promoter of each gene contained over-represented octamer units, which appeared frequently in the *stop1*-repressed genes [relative appearance ratio (RAR) >5; Supplementary Fig. S3]. For each gene, the promoter region harboring the GGNVS consensus sequence was labeled as CIS1 (and CIS 2 for promoters with two GGNVS motifs; Supplementary Fig. S3; Table S3). This resulted in the identification of eight candidate regions in the promoters of a total of six genes. These candidate STOP1-binding motifs were then tested using an *in vitro* competitive assay based on an amplified luminescence proximity homogeneous assay (AlphaScreen) system (Fig. 2B). The AlphaScreen system can detect the interaction between a FLAG-tagged protein and biotinylated double-stranded DNA (dsDNA), using the anti-FLAG antibody and streptavidin coated beads. The competitive AlphaScreen was used to evaluate STOP1-binding capacity of predicted CIS regions by the inhibition of the binding of STOP1 protein with the dsDNA for the GGNVS consensus region previously identified in the *AtALMT1* promoter and labeled as CIS-D (*ALMT1*-CIS-D; containing a functional STOP1-binding site; Tokizawa *et al.*, 2015). Competitive binding assays were carried out on the eight predicted STOP1-binding sequences found in the promoters of the six genes identified in Supplementary Fig. S3. It was found that STOP1 binding was strongly inhibited using *GDH2* (*GLUTAMATE-DEHYDROGENASE2*)-CIS1 and *STOP2*-CIS1, and weakly inhibited with *AtMATE*-CIS1 (Fig. 2B). Additionally, *GDH2*-CIS1 and *STOP2*-CIS1 regions generated an AlphaScreen signal that was comparable with that seen in *ALMT1*-CIS-D (Fig. 2C). Furthermore, mutation of the STOP1-binding region in *GDH2*-CIS1 and *STOP2*-CIS1 suppressed the binding of STOP1 *in vitro* (Supplementary Fig. S4).

### *Functional and comparative analyses of the STOP1-binding site in the* GDH2 *and* STOP2 *promoters*

To investigate whether the identified STOP1-binding sites in the *AtMATE*, *GDH2,* and *STOP2* promoters were functional, *in planta* promoter assays using promoter::*GUS* transgenic plants were conducted. Mutations in the STOP1-binding sites in the *GDH2* and *STOP2* promoters led to lower gene expression after a 24 h period of root exposure to control or Al-containing solutions, but this did not occur using *AtMATE* (Fig. 3A). Additionally, Al-inducible expression of *GDH2* and *STOP2* were suppressed by mutating the STOP1-binding site in their promoters, based on *GUS* expression.

To confirm *in vivo* interaction of STOP1 with its target promoters, we conducted chromatin immunoprecipitation-quantitative PCR (ChIP-qPCR) analysis between STOP1 and the *AtALMT1*, *GDH2,* and *STOP2* promoters (Fig. 3B). The roots of Col-0 and transgenic plants expressing the *STOP1* promoter::STOP1-GFP were treated with 10 μM $AlCl_3$ for 1.5 h and 6 h, or without Al (i.e. 0 h), and then these samples were subjected to ChIP-qPCR analysis. The amount of DNA in both the before/after immunoprecipitation samples (i.e. input and IP sample) was measured by real-time qRT-PCR. Three different primer sets (P1-P3) were designed for the *AtALMT1*, *STOP2*, and *GDH2* promoters. The P2 primer set in each gene was designed to cover the identified STOP1 binding site, and P1 and P3 primers were located upstream and downstream from the binding site, respectively (Fig. 3B). The DNA in *Mutator-like transposon* loci (*Mu-like*) was measured as a negative control. Any significant difference ($P \geq 0.05$, Student's *t*-test) in enrichment was not observed in the loci between transgenic plants and Col-0. However, the P2 regions for the three target genes were significantly enriched ($P < 0.01$, Student's *t*-test) in the transgenic plants, especially after Al treatment, while the P1 and P3 regions in each gene promoter did not yield an enrichment. However, this enrichment does not increase at the 6 h time point in comparison with the 1.5 h Al treatment, in all promoters.

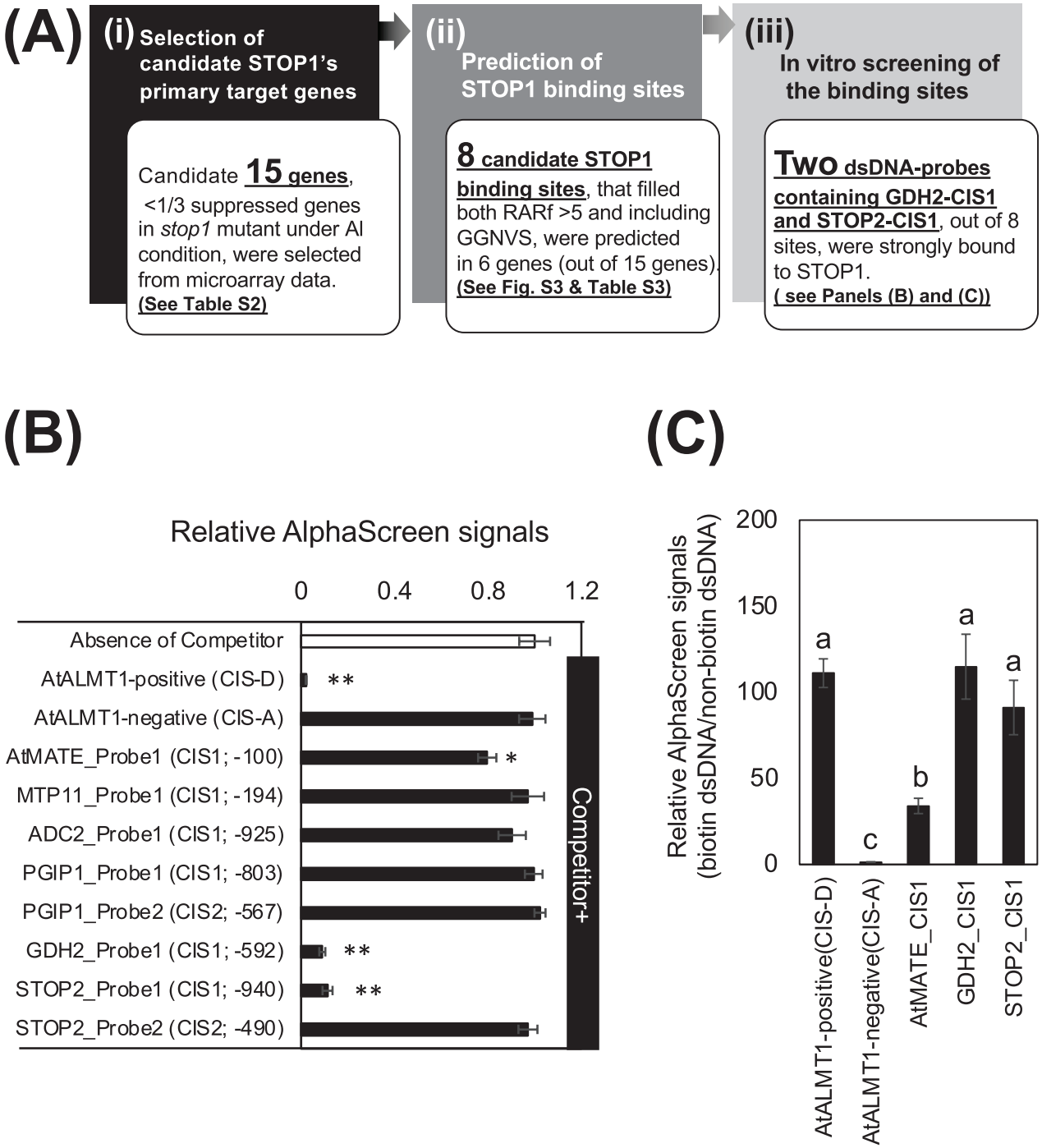


**Fig. 2.** Identification of *in vitro* STOP1 interactions with *cis*-acting elements in the promoters of STOP1-regulated genes. (A) Schematic representation of the procedures used to identify *cis*-acting elements that interact with STOP1 in the promoters of STOP1-regulated genes. (B) Competitive AlphaScreen assay of putative STOP1-interacting *cis*-acting elements in the promoters of STOP1-regulated genes. The putative STOP1-binding sites were predicted by *in-silico cis*-element prediction assays (Supplementary Fig. S3; Table S3). The dsDNA probes, which were 30–34 bp long sequences including the putative STOP1-binding sites (Supplementary Table S4), were analysed in terms of their ability to compete with STOP1 for the STOP1-binding site in the *AtALMT1* promoter (CIS-D). Positions of the putative STOP1-binding sites from the transcription start site are shown. The biotinylated *AtALMT1* CIS-D probe was incubated with ten-fold higher concentrations of a series of unlabeled competitive probes in the AlphaScreen reactions, which generate AlphaScreen signals because of the binding of STOP1 to biotinylated *AtALMT1* CIS-D. Competing probes decrease the AlphaScreen signals. Data are presented as the mean relative AlphaScreen signal (absence of competitor was set as 1) ±SD ($n$=3). Asterisks indicate a significant difference from the data in the absence of a competitor (*$P$<0.05, and **$P$<0.01; Student's $t$-test). (C) *In vitro* chemiluminescence assay for evaluating the binding capacity of promoter regions containing *AtMATE*-CIS1, *GDH2*-CIS1 and *STOP2*-CIS1 sequences with positive (*AtALMT1* positive; containing CIS-D, which binds to STOP1 under the same experimental conditions; Tokizawa *et al.*, 2015) and negative (*AtALMT1* negative; containing the promoter region that does not interact with STOP1) controls. Relative AlphaScreen signals (chemiluminescence of a reactive biotinylated dsDNA probe relative to that of non-reactive unlabeled control dsDNA) were analysed for each promoter region. Data are presented as the mean ±SD ($n$=4). Different letters indicate a significant difference ($P$<0.05, Tukey's test).

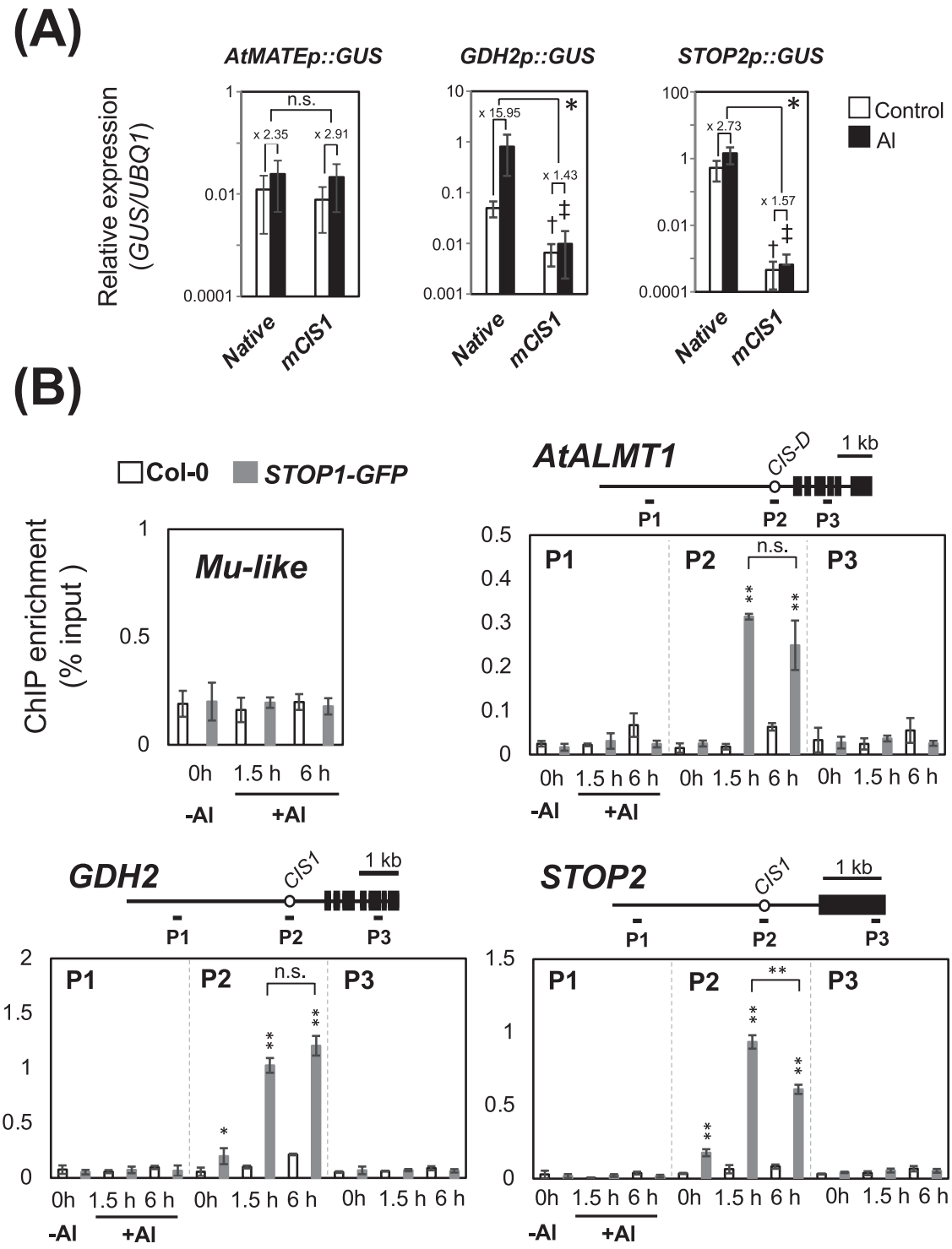


**Fig. 3.** *In planta* identification of functional STOP1-binding sites. **(A)** *GUS* expression (Control or 10 μM $AlCl_3$, 24h) in transgenic *A. thaliana* plants carrying the *AtMATE* promoter*::GUS (AtMATEp::GUS)*, *GDH2* promoter*::GUS* and *STOP2* promoter*::GUS* with or without a mutation in *AtMATE*-CIS1, *GDH2*-CIS1 and *STOP2*-CIS1 (Fig. 2). *GUS* expression was quantified in at least five different independent transgenic lines. Data are presented as the mean relative expression as a base-10 logarithmic scale (normalized against *UBQ1* expression) ±SD ($n \geq 5$). Dagger and double dagger indicate a significant difference from the native promoter's expression in control and Al conditions, respectively, and asterisk indicates a significant difference in fold-induction (Al/Control) between the native and the modified promoter (†, ‡, or *$P<0.05$, Student's *t*-test). n.s., no significant difference. (B) Chromatin immunoprecipitation-quantitative PCR (ChIP-qPCR) analysis using transgenic plants expressing *STOP1* promoter*::STOP1-GFP* was conducted for *AtALMT1*, *GDH2*, *STOP2*, and *Mutator-like transposon* (*Mu-like*, negative control for the experiment) loci. Upper panel in each graph depicts a schematic diagram of the gene structure, position of identified *in vitro* STOP1 binding site (white circle, Fig. 2), and amplified regions in ChIP-qPCR. Col-0 and

### *Al-responsive expression patterns for genes harboring the STOP1 binding* cis*-element*

When 10 day-old seedlings grown in control medium were exposed to a solution containing 10 μM $AlCl_3$, the expression of *AtALMT1*, *GDH2* and *STOP2* was up-regulated at 1 h and 1.5h (Fig. 4A). This short-term Al-induced gene transcription was very strongly inhibited in a T-DNA insertion knock-out mutant of STOP1 (*STOP1*-KO; Fig. 4B). In addition, mutation of the STOP1-binding region in the *AtALMT1*, *GDH2* and *STOP2* promoters (i.e. mCIS-D in *AtALMT1*, and mCIS-1 in *GDH2* and *STOP2*) suppressed this early Al-induced expression (1.5 h Al treatment) via the *in planta* promoter:*GUS* assays (Figs 1B; 4C). Al-inducible expression of *AtALMT1* and *GDH2* continued to increase after 1.5 h in Al treatment, but this did not occur for *STOP2* expression. Additionally, Al-induced *STOP2* expression was much lower than that of the other genes (Fig. 4A). These results indicate that different or additional transcriptional regulatory mechanisms are involved in Al-inducible expression of *STOP2*, compared with *AtALMT1* or *GDH2*. In addition, Al-induced expression of *AtMATE* and *ALS3* occurred at 3 h and 6 h after initiating the Al treatment (Fig. 4A), and this induction was also suppressed in the *STOP1*-KO (Fig. 4D).

### *STOP1 directly regulates Al-induced* AtMATE*, but not* ALS3 *expression*

The above-mentioned analyses identified that Al-induction of *AtMATE* and *ALS3* expression was observed, but only at 3–6 h of Al treatment (Fig. 4A). This Al induction was delayed compared with genes like *AtALMT1* and *GDH2,* but it is STOP1-dependent (Fig. 4D). We identified STOP1 binding sites in *AtMATE* promoter by prediction methods combined with *in silico* binding assay (*AtMATE*-CIS1 in Fig.2), but the mutation in the binding site did not suppress the promoter activity *in vivo* (Fig. 3A), suggesting that other STOP1-binding sites may be involved in the regulation. Based on DNA affinity purification sequencing (DAP-seq) analysis by O'Malley *et al*. (2016), we found another possible STOP1-binding region in the *AtMATE* promoter (gray shaded regions in Fig. 5A, GEO accession number: GSE60143). A significant enrichment ($P<0.05$, Student's *t*-test) by ChIP-qPCR was observed for the D1 region after a 6 h Al treatment (Fig. 5A); D1 overlaps with the DAP-seq peaks in the *AtMATE* promoter. On the other hand, ChIP-qPCR for the D2 region (close to CIS1 region of *AtMATE* promoter) did not show significant enrichment. This suggests that CIS1 a has lower affinity to interact with STOP1 *in vivo*.

An *in planta* promoter deletion assay revealed that Al-inducible *ALS3* expression involves an Al-responsive promoter region at −138 to −238 bp from the ATG start codon (Fig. 5B). Although none of the over-represented octamer units associated with *stop1*-suppressed genes were identified (Supplementary Fig. S3), octamer units found in Al-inducible genes (CIS-Y and Z in Fig. 5C) were identified in the *ALS3* promoter (−138 to −238 bp from the ATG). The CIS-Y mutation inhibited Al-inducible gene expression (Fig. 5D). This site is closely located to the DAP-seq positive region (–160 to +41 from ATG, gray shaded regions in Fig. 5A), but was unable to bind to STOP1 in both *in vivo* and *in vitro* analysis (Fig. 5A, E). These results confirm that STOP1 indirectly regulates Al-induced *ALS3* expression in the relatively early stages (up to 6 h) of Al treatment.

### *Comparison of STOP1-binding sequences in the target genes*

The *AtALMT1* STOP1-binding site sequence was analysed in an *in vitro* competitive binding assay, and then compared with the STOP1 binding on the *GDH2*-CIS1, *STOP2*-CIS1, and *AtMATE*-CIS2 sequences. *AtMATE*-CIS2 was identified based on DAP-seq/ChIP-qPCR analysis in Fig. 5A. The competitor probes in which a single nucleotide mutation decreased the STOP1 binding produced a greater AlphaScreen signal than the native unmutated sequence during the *in vitro* competitive binding assay (Fig. 6A). We found that 10 nucleotides among 15 bp-long sequence in the STOP1-binding site of *AtALMT1* (indicated by white font; Fig. 6A) are important for STOP1 binding. Almost all these important nucleotides for the binding were also present in the STOP1-binding sequences of *GDH2*-CIS1, *STOP2*-CIS1, and *AtMATE*-CIS2 (Fig. 6B). Our *in vitro* binding assay showed that there was no significant difference ($P\geq0.05$, Tukey's test) between the affinity of STOP1 with *ALMT1*-CIS-D, *GDH2*-CIS1, or *STOP2*-CIS1 binding sequences (Fig. 2C). However, the binding affinity of STOP1 with *AtMATE*-CIS2 binding sequence was significantly lower ($P<0.05$, Tukey's test) than that with *ALMT1*-CISD and *GDH2*-CIS1 sequences (Fig. 6C).

### *Phosphoinositide pathway enzymes are involved in early STOP1 nuclear accumulation and Al-inducible expression of STOP1 target genes*

In this study, we found that the STOP1 nuclear localization and transcriptional activation of the target genes were observed within 1.5 h of Al treatment. Our recent study

*STOP1* promoter::*STOP1-GFP* seedlings (10 day-old) were treated with 10 μM $AlCl_3$ for 1.5 h and 6 h, or without $AlCl_3$ (0 h). Chromatin extracted from the root samples was collected by immunoprecipitation assay using an anti-GFP antibody. The abundance of DNA was determined by quantitative real-time PCR (qRT-PCR) using specific primer sets (Supplementary Table S1). The enrichment of PCR products from immunoprecipitated DNA was normalized with the corresponding input DNA. Data are presented as the mean ±SD ($n=3$). Asterisks indicate a significant difference between Col-0 and *STOP1* promoter::*STOP1-GFP*, or 1.5 h or 6 h $AlCl_3$ treatment in the transgenic plants (*$P<0.05$, and **$P<0.01$; Student's *t*-test).

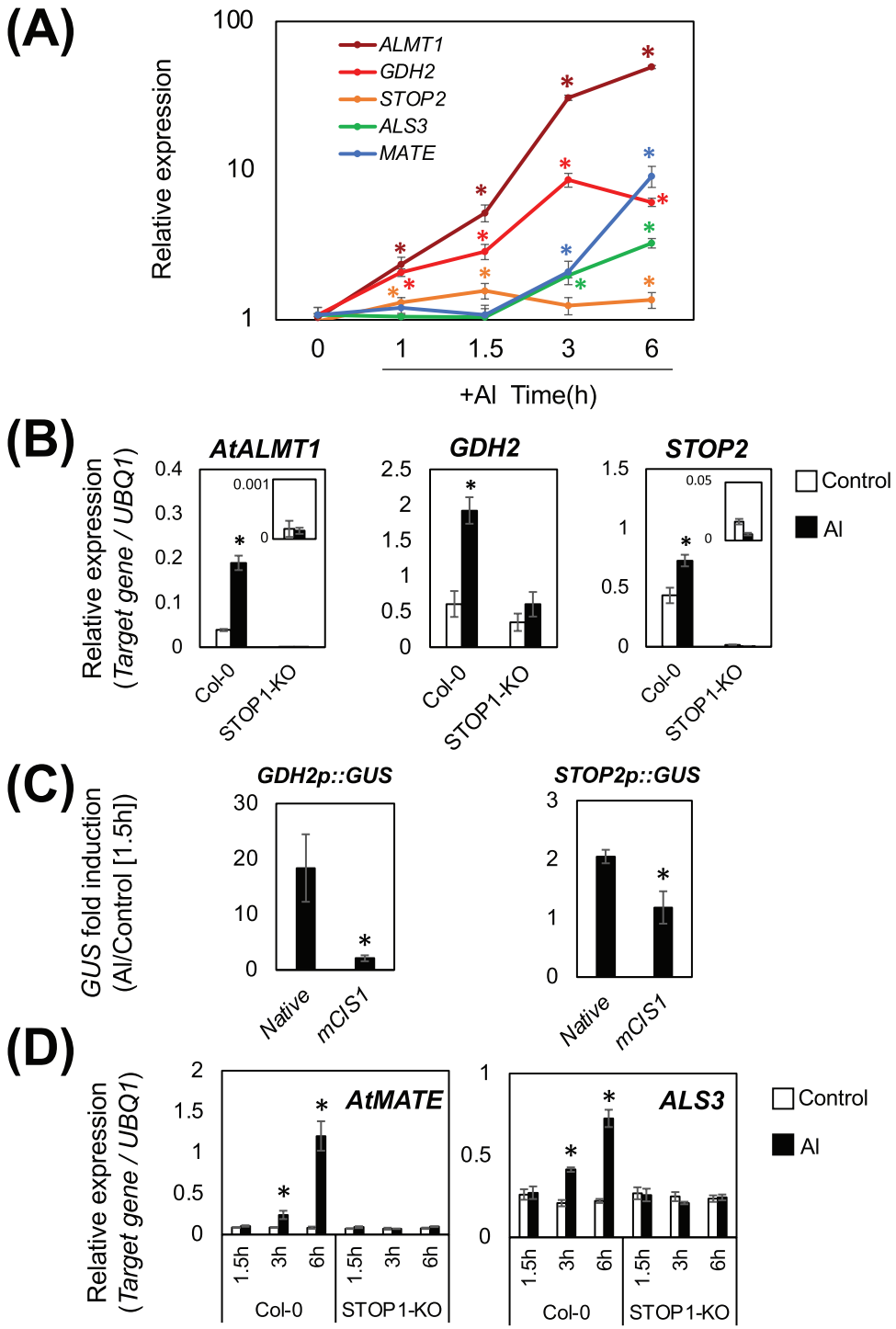


**Fig. 4.** Gene expression profile of STOP1-regulated genes under Al treatment. (A) Time course of Al-inducible expression of *AtALMT1*, *GDH2*, *STOP2*, *ALS3*, and *AtMATE*. The transcript abundance of each gene was determined by quantitative real-time PCR (qRT-PCR) and normalized against *UBQ1* expression. Relative values (values at time 0 were set as 1) are shown in panel (A). Data are presented as the mean ±SD ($n$=3). Asterisks indicate a significant difference compared with the data for time 0 (*$P$<0.05, Student's $t$-test). (B) Short-term (1.5 h) inducible expression of *AtALMT1*, *GDH2*, and *STOP2* in Col-0 and *STOP1*-KO plants, which were incubated in 10 μM $AlCl_3$. Data are presented as the mean ± standard deviation (n = 3). Asterisks indicate a significant difference between the control and treatments (*$P$ < 0.05; Student's $t$-test). (C) Short-term (1.5 h) Al-responsive *GUS* expression in transgenic *A. thaliana* carrying *GDH2* promoter*::GUS* (*GDH2p::GUS*) and *STOP2* promoter*::GUS*, with or without a mutation in *GDH2*-CIS1, and *STOP2*-CIS1 (Fig. 2). Data are presented as the mean ±SD ($n$≥5). Asterisks indicate a significant difference from the *GUS* fold induction in native promoter (*$P$<0.05; Student's $t$-test). (D) Expression of *AtMATE* and *ALS3* in the roots of Col-0 and *STOP1*-KO in the presence or absence of 10 μM $AlCl_3$. *ALS3* and *AtMATE* expression was determined by qRT-PCR using *UBQ1* expression as the internal control. Data are presented as the mean ±SD ($n$=3). Asterisks indicate a significant difference from the expression in control (*$P$<0.05; Student's $t$-test).

showed that chemical inhibitors of key enzymes involved in the phosphoinositide (PI) metabolic pathway, phenylarsine oxide (PAO) [i.e., phosphatidylinositol-4-kinase (PI4K) inhibitor] and U73122 [i.e., phospholipase C (PLC) inhibitor], inhibit Al-induced transcription of *AtALMT1* and other Al-inducible genes including *AtMATE* and *ALS3* during a 3 h Al treatment (Wu *et al.*, 2019). In the PI pathway, PI4K produces phosphatidylinositol-4-phosphate (PI4P) from PI and PLC produces inositol 1,4,5-trisphosphate ($IP_3$) from $PI(4,5)P_2$ (Fig. 7A). To clarify whether these inhibitors block the early (1.5 h) Al responses, we analysed their effect on STOP1-nuclear localization and the transcriptional activation of the primary target genes during the 1.5 h Al exposure. To minimize unexpected side-effects from the inhibitors, we used the inhibitors for PI4K and PLC at lower concentrations than what were used in several previous studies (Parre *et al.*, 2007; Fujimoto *et al.*, 2015; Riveras *et al.*, 2015; Takahashi *et al.*, 2017; Rubilar-Hernández *et al.*, 2019). STOP1 nuclear localization was supressed by PAO and U73122, but not by LY294002 (a PI3K inhibitor) and U73343 (the structural analog of U73122) (Fig. 7B). In addition, Al-induced *AtALMT1* and *GDH2* expression was significantly suppressed ($P<0.05$, Student's *t*-test) by PAO and U73122, but not by LY294002 and U73343 (Fig. 7C). Interestingly, LY294002 actually enhanced Al-induced *AtALMT1* and *GDH2* expression. On the other hand, STOP1 expression was not changed by these inhibitors. These results suggest that the effect of these inhibitors is on post-transcriptional regulation of STOP1 (i.e. nuclear localization), and subsequently this leads to the reduction of *AtALMT1* and *GDH2* transcription (Fig. 7C). Additionally, Al-induced *STOP2* expression was also significantly suppressed ($P<0.05$, Student's *t*-test) by U73122 and 2 μM PAO (Supplementary Fig. S5). However, LY294002 also inhibited *STOP2* expression unlike *AtALMT1* and *GDH2* expression, suggesting that Al-induced activation of STOP2 involves a different mechanism.

### GDH1 *and* GDH2 *contribute to Al tolerance in Arabidopsis*

In the present study, we identified that STOP1 directly regulates the early Al-inducible expression of *GDH2* and *STOP2,* and *AtALMT1*. Previous reports showed that the reduced Al tolerance of *stop1* mutants recover to a degree by expressing *STOP1* promoter::STOP2, due to the partial recovery of *ALS3* and *AtMATE* expression (Kobayashi *et al.*, 2014). However, prior to this study there was no evidence that *GDH* contributes to Arabidopsis Al tolerance. There are three *GDH* homologues in Arabidopsis, and root GDH activity is strongly inhibited by mutation of *GDH1* and *GDH2* (Fontaine *et al.*, 2012). In addition to *GDH2*, *GDH1* expression was also induced by 1.5 h Al treatment, and this expression was supressed in the *STOP1-KO* (Fig. 8A). The direct binding of STOP1 to the *GDH1* promoter was observed in both *in vivo* and *in vitro* interaction assays (Fig. 8B, C), and the STOP1 binding affinity to the *GDH1* promoter was almost the same as its binding to the *AtALMT1* promoter (Fig. 8C). Additionally, the *GDH1* promoter also has a conserved STOP1 binding sequence similar to other target genes (Supplementary Fig. S6). These results indicate that STOP1 directly regulates the expression of both *GDH1* and *GDH2* under Al stress conditions. Therefore, we examined Al sensitivity in T-DNA insertion mutants of *gdh1, gdh2,* and *gdh1/2* (double mutant) (Fig. 8D). Under 4 μM $AlCl_3$ stress, severe root growth inhibition was observed in the *STOP1-KO*. Additionally, *gdh2* was Al-sensitive but this was not the case for *gdh1*. However, Al-sensitivity was increased in the *gdh1/2* double mutant, suggesting both GDH1 and GDH2 are involved in Al tolerance.

## Discussion

Al-induced transcription of *AtALMT1* is rapidly induced by Al within 1 h (Kobayashi *et al.*, 2007; Ding *et al.*, 2013) and is a critical step for Al-responsive root malate exudation, the major Arabidopsis Al tolerance mechanism (Hoekenga *et al.*, 2006; Kobayashi *et al.*, 2007). In this study, we identified the molecular mechanism for Al-induced early STOP1-mediated expression of target genes, including *AtALMT1* (Fig. 9). Our cytochemical analysis confirmed that STOP1 protein accumulated in the nucleus soon after Al treatment (within 1.5 h). Nuclear STOP1 accumulation and increased *AtALMT1* expression were also observed under CHX treatment (Fig. 1E, F). These results indicate that some type of post-translational regulation is involved in the early Al activation of *AtALMT1* expression. Under control conditions (i.e. without Al), expression of *STOP2* and *GDH1* were suppressed in the STOP1-KO (Figs 4B; 8A), and the significant enrichment of DNA containing the STOP1 binding region in these genes was observed by ChIP assay (Figs 3B; 8B). These results indicate that STOP1 should be functional and exist in the nucleus under control conditions. However, the STOP1-GFP proteins were mainly observed as small dots in the cell under control conditions (Fig. 1D). We analysed fluorescence images generated for the double transgenic lines carrying the genes encoding STOP1-GFP and mCherry-tagged organelle marker proteins, and under control conditions, STOP1 protein localized not only in the nucleus but also in the Golgi apparatus (Supplementary Fig. S7). This result suggests that Golgi-localized STOP1 proteins may contribute towards rapid nuclear accumulation in response to Al. Because STOP1 lacks a membrane-spanning domain, it relies on another mechanism to remain in the Golgi apparatus. Further research will be needed to clarify how STOP1 is retained in the Golgi apparatus under control conditions, and how they can be released and localized to the nucleus. Based on fluorescence signals, the Al-regulated nuclear accumulation of STOP1-GFP decreased in the presence of CHX 6 h after

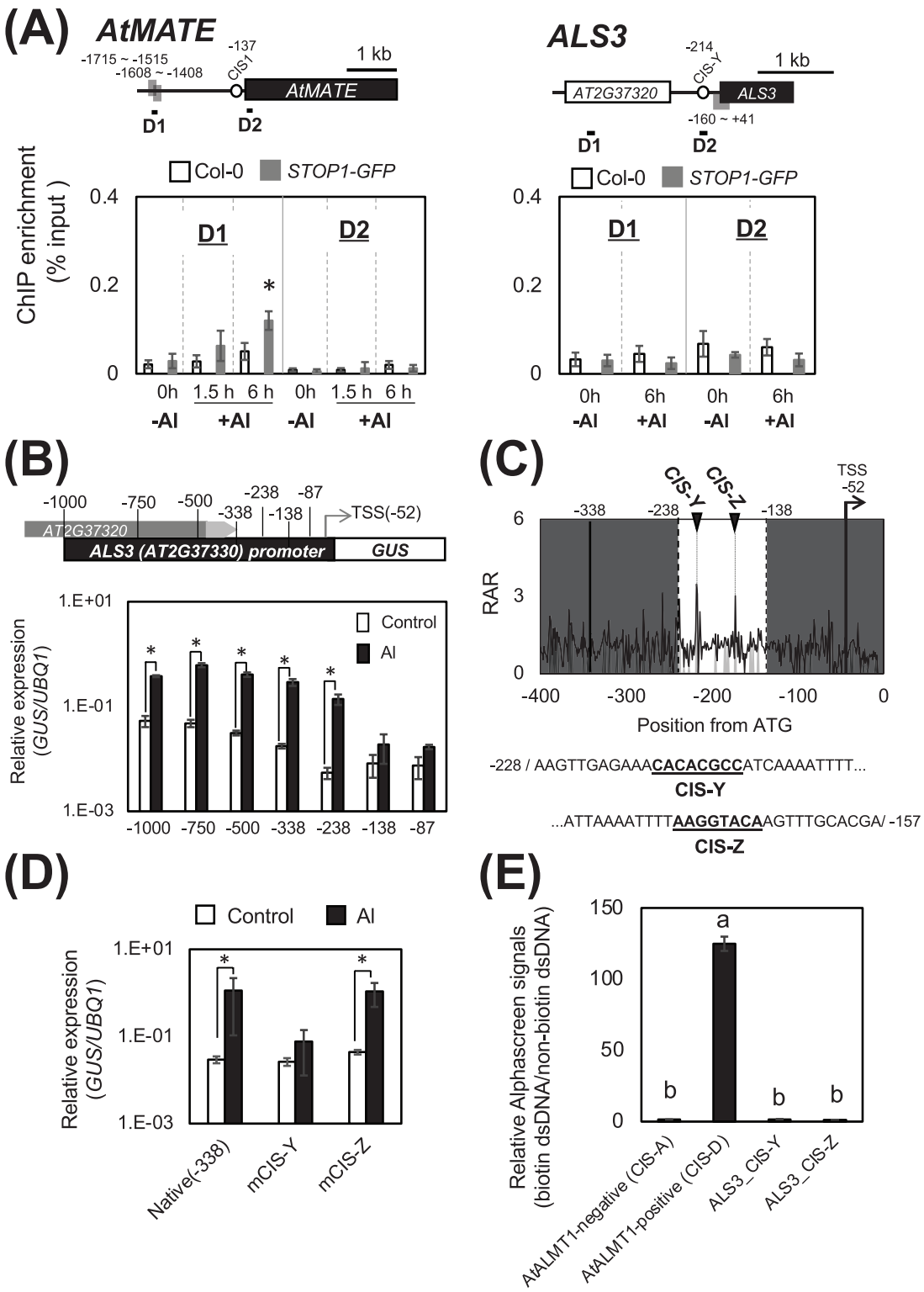


**Fig. 5.** Characterization of promoter elements in the *AtMATE* and *ALS3*. (A) Chromatin immunoprecipitation-quantitative PCR (ChIP-qPCR) assay on *AtMATE* (left) and *ALS3* loci (right) using transgenic plants carrying the *STOP1* promoter::*STOP1-GFP*. Schematic diagrams of *AtMATE* and *ALS3* loci are shown (upper panels). Gray shaded boxes indicate potential STOP1 binding promoter regions which were identified by *in vitro* ChIP-seq analysis (DAP-seq, O'Malley *et al.*, 2016). The amplified regions by ChIP-qPCR analysis are shown as D1 and D2 (Supplementary Table S1). Data are presented as the mean ±SD ($n$=3). The immunoprecipitated DNA by anti-GFP antibody was normalized against the input DNA. Asterisks indicate a significant difference

initiating Al treatment (Fig. 1E). This suggests that STOP1 proteins are eventually degraded, while newly synthesized STOP1 proteins help to maintain Al-responsive *AtALMT1* expression in the longer-term phase. In fact, STOP1 has a relatively fast predicted turnover rate, with a half-life of 5–31 h as predicted by the TermiNator 3 program (https://bioweb.i2bc.paris-saclay.fr/terminator3; Martinez *et al.*, 2008).

Zhang *et al.* (2019) reported that RAE1 promotes degradation of STOP1 proteins under control and Al conditions. Interestingly, in the *rae1* mutant, STOP1 protein amounts were much higher than wild type Col-0 under control conditions. These results indicate that STOP1 protein is ubiquitously transcribed, and RAE1 contributes to the low amount of STOP1 nuclear localization and *AtALMT1* expression under control conditions via the ubiquitin-26S proteasome pathway. Additionally, it has been shown that HPR1 mediates STOP1 mRNA export from the nucleus and an *HPR1* mutant increases STOP1 mRNA retention in the nucleus which ultimately results in reduced STOP1 protein abundance (Guo *et al.*, 2020). These results indicate that multiple mechanisms controlling mRNA export, protein degradation, and protein localization work together to control STOP1 protein abundance and its nuclear accumulation. This complex regulation of STOP1 protein abundance might contribute to the involvement of STOP1 in response to different environmental stresses, and explain why *AtALMT1* expression can be induced by several stimuli and signals.

Our *in vitro* binding assays revealed that the 15 bp-long sequence (GGGGAGGGCTTAACT, Fig. 6A) in the *AtALMT1* promoter was the minimum sequence for STOP1 binding, which is much longer than the consensus sequence of the binding site of STOP1-like ART1 proteins (i.e. GGNVS). To examine from the aspect of protein structure, whether STOP1 protein can bind to such a long sequence, we generated a homology-based topology model of the STOP1-*ALMT1* (CIS-D) transcriptional module. The model was developed using a well-characterized mouse zinc finger transcription factor ZFP568 as a template (Patel *et al.*, 2018), using the YASARA modeling program (Krieger and Vriend, 2014). As expected, in our model, STOP1 bound to the *AtALMT1* CIS-D regulatory element (Supplementary Fig. S8). The amino acid residues involved in folding of the four zinc fingers were closely located with the required nucleotides for the STOP1-*AtALMT1* promoter interaction, which is consistent with our previous result showing that all four zinc finger domains in STOP1 are essential for binding to the *AtALMT1* promoter (Tokizawa *et al.*, 2015). These insights into the structure of STOP1/*AtALMT1* module further supports our experimental results that STOP1 recognizes the long *cis*-element, and helps to elucidate the molecular structure of STOP1 binding. In addition to activating *AtALMT1* expression, Al-induced STOP1 accumulation in the nucleus also activated the transcription of *STOP2*, *GDH1* and *GDH2*, which also harbor a long STOP1-binding sequence similar to that of the *AtALMT1* promoter (Fig. 6B).

We identified the *in vitro* STOP1 binding site (*AtMATE*-CIS1, –137 bp from the translation initiation site) on the *AtMATE* promoter by *in silico* promoter element prediction method (Fig. 2). Mutation in this region does not clearly affect the *in vivo* promoter activity (Fig. 3A). One possibility would be regulation by other STOP1-regulated sites in the upstream promoter region. In fact, DAP-seq data analysis identified another STOP1-binding site, *AtMATE*-CIS2 (–1597 bp from the translation initiation site), in the promoter (Figs 5A; 6B). Interestingly, *AtMATE* expression was not induced during a 1.5 h Al treatment. Our *in vitro* binding assay showed that the binding affinity of STOP1 with the *AtMATE*-CIS2 was significantly lower than that of the primary STOP1 target genes (Fig. 6C). In addition, a methylome analysis on the root tips of Arabidopsis revealed that the site(s) for DNA methylation were not detected near the STOP1-binding site in the *AtMATE* promoter [Supplementary Fig. S9; Kawakatsu *et al.*, (2016); http://neomorph.salk.edu/Arabidopsis_root_methylomes.php], suggesting that a demethylation process is not involved in the delayed *AtMATE* activation. Therefore, the weak binding affinity of STOP is probably the reason for the longer Al exposure period needed to induce *AtMATE* expression (3 h). This is supported by our ChIP results showing that the STOP1 binding region in the *AtMATE* promoter was not significantly

between Col-0 and *STOP1* promoter::*STOP1-GFP* (*$P$<0.05; Student's *t*-test). (B) Aluminum-inducible expression of *GUS* in transgenic *A. thaliana* plants carrying the *ALS3* promoter::*GUS* (–1000 bp from the ATG start codon) and a series of 5'-deleted promoter::*GUS*. Transgenic seedlings were treated with or without 10 μM $AlCl_3$ for 6 h, and *GUS* expression was analysed by quantitative real-time PCR (qRT-PCR). Asterisks indicate a significant difference from the control level (*$P$<0.05, Student's *t*-test). Data are presented as the mean ±SD (n≥4). (C) Predicted Al-responsive *cis*-acting elements in the *ALS3* promoter. The relative appearance ratio of octamers in the *ALS3* promoter was plotted (i.e. over-representation in Al-inducible genes; see Materials and Methods section). Gray-shaded regions represent significantly over/under-represented octamers ($P$<0.05, Fisher's exact test). The promoter region in white corresponds to –138 to –238 bp from the ATG start codon. This region includes the Al-responsive *cis*-acting elements [see panel (B)]. (D) Evaluation of Al-responsive *cis*-acting elements in the *ALS3* promoter. Aluminum-inducible expression of *GUS* in transgenic *A. thaliana* carrying the native *ALS3* promoter (0 to –338 bp from the ATG start codon) or promoters with a mutated CIS-Y or CIS-Z sequence. *GUS* transcript abundance in the roots treated with a control solution (no Al) or 10 μM $AlCl_3$ for 6 h was analysed by qRT-PCR. Data are presented as the mean ±SD ($n$≥4). Asterisks indicate a significant difference between the control and $AlCl_3$ treatments (*$P$<0.05, Student's *t*-test). (E) The *in vitro* binding capacities of CIS-Y and CIS-Z for STOP1 were compared with the positive control (i.e. STOP1-binding CIS-D region of the *AtALMT1* promoter) and negative control (i.e. CIS-A region of the *AtALMT1* promoter; Tokizawa *et al.* 2015). The chemiluminescence generated from the interaction between STOP1 protein and the double-stranded DNA (dsDNA) probes was detected by AlphaScreen system. The relative signals indicate ratio of chemiluminescence intensity of a reactive biotinylated dsDNA probe and that of non-reactive unlabeled control dsDNA. Data are presented as the mean ±SD ($n$=3). Different letters indicate a significant difference ($P$<0.05, Tukey's test).

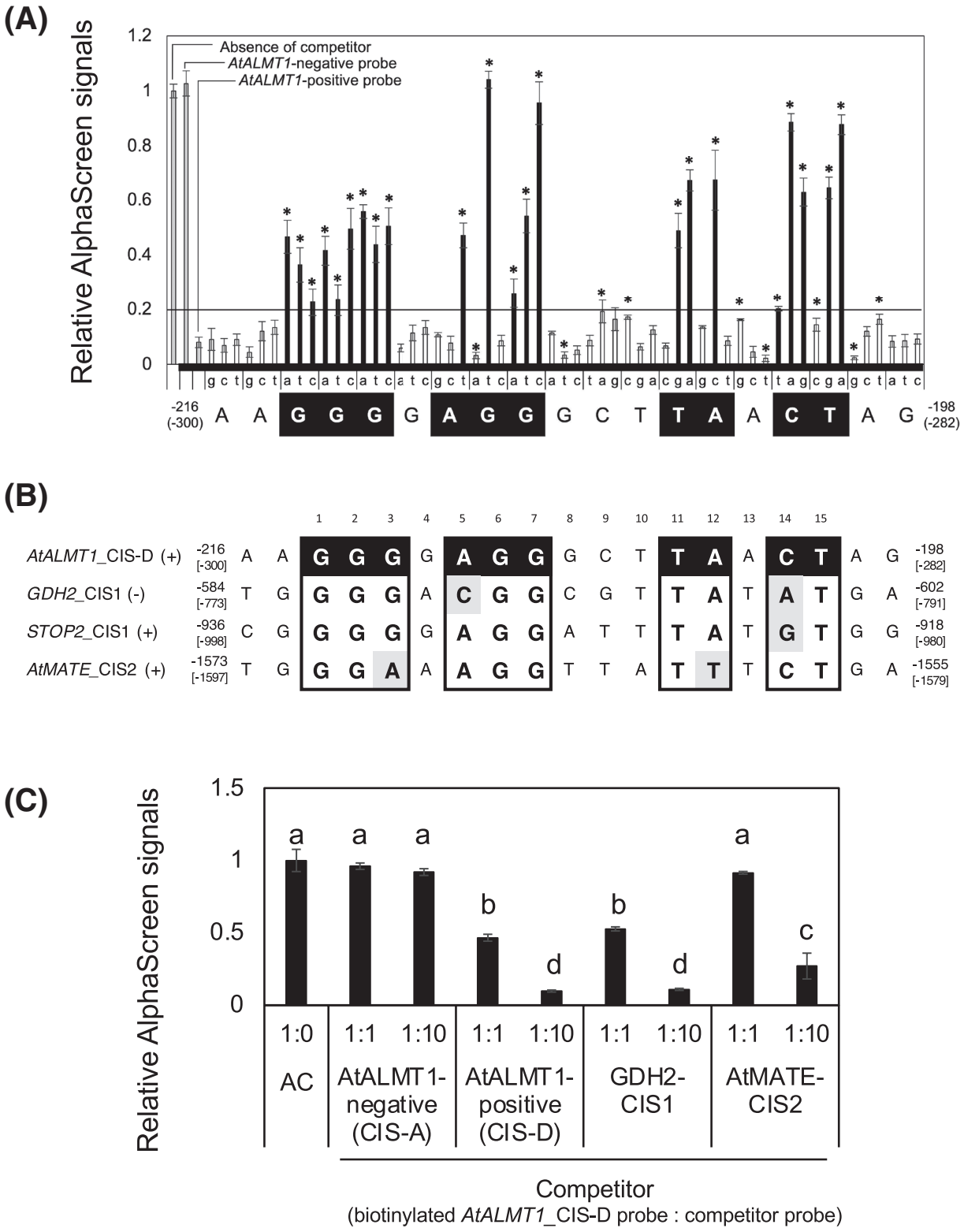


**Fig. 6.** Comparison of conserved STOP1-binding sequence in the target genes. (A) Effect of a single nucleotide mutation on the binding capacity of the *AtALMT1* promoter CIS-D region, which binds to STOP1. The native *AtALMT1* promoter sequences are indicated by capital letters below the graph. AlphaScreen signals were analysed in a competitive assay involving 30 bp reactive dsDNA (biotinylated CIS-D probe) with a single nucleotide substitution (shown as small letters above the native *AtALMT1* sequences) at a 1:10 molar ratio. Data are presented as the mean ±SD ($n$=4). Asterisks indicate a significant difference (*$P$<0.01, Student's $t$-test). A higher relative AlphaScreen signal (RAS) indicates the mutation decreased STOP1 binding. Black

enriched after 1.5 h Al treatment, but was after 6 h of Al exposure (Fig. 5A). In addition, our promoter analysis for *ALS3* identified a promoter element that is responsible for Al-induced transcription, but STOP1 did not bind in this region both *in vitro* and *in vivo* (Fig. 5A, E). Additionally, Al-activation of *ALS3* transcription was slower (required at least 3 h Al exposure), compared with the more rapid Al-induced activation of transcription for the primary STOP1 target genes such as *AtALMT1* (Fig. 4A). These results indicate that there may be other transcription factors which are regulated by STOP1 and are directly involved in the expression of *ALS3*. Identification of these transcription factors will help further clarify the complex mechanisms underlying the transcriptional regulation of Al-tolerance genes.

The accumulation of STOP1 in the nucleus may explain the short-term Al-inducible expression of *AtALMT1* (i.e. within 1.5 h; Fig. 4A). However, other mechanisms are required to explain the longer-term Al-induced expression, including the regulation of the *AtALMT1* transcriptional activator (i.e. CAMTA2; Tokizawa *et al.*, 2015) and repressor (i.e. WRKY46; Ding *et al.*, 2013). Similar to *AtALMT1*, Al-inducible *GDH1* and *GDH2* expression was increased after 1.5 h of Al exposure (Figs 4A; 8A). This longer-term Al-inducible expression of these genes would be regulated by other transcription factors. For example, W-box motifs, a binding motif of WRKY-type transcription factors (Eulgem *et al.*, 2000; Sun *et al.*, 2003), were found in the *GDH 1* and *GDH2* promoters, and a CGCG box domain, a CAMTA family protein binding motif (Yang and Poovaiah, 2002), was found in the *GDH2* promoter by *in silico* promoter elements analysis using New PLACE (Plant *cis*-acting regulatory element database; Higo *et al.*, 1999; Supplementary Table S5). In addition, several studies reported that the BASIC-LEUCINE-ZIPPER 1 (bZIP1, AT5G49450) transcription factor regulates *GDH1* and *GDH2* expression (Dietrich *et al.*, 2011; Para *et al.*, 2014). Because the expression of *bZIP1* was induced by Al [Fold-change (10 μM $AlCl_3$ /control, 24 h) =4.01, microarray data from Tokizawa *et al.*, 2015], bZIP1 transcription factors may be involved in the Al-induced expression of *GDH* genes. In addition, several ACGT-based motifs, a binding motif of bZIP-type transcription factor (Foster *et al.*, 1994; Kang *et al.*, 2010), were found in these promoters (Supplementary Table S5). Our expression analysis on *GDH2* showed that expression was significantly supressed in the *STOP1-KO*, but was still higher than *AtALMT1* and *STOP2* expression (Fig. 4B). However, *GDH2* promoter activity was almost abolished when the STOP1-binding region was mutated (Fig. 3A). In our promoter::reporter assay, 1 kb promoter region upstream of the translational start site in *GDH2* was used for the evaluation of promoter activity, suggesting that other regions (e.g. promoter region upstream of 1 kb) may also be involved in the expression. In fact, several W-box, CGCG box, and ACGT motifs were found in the *GDH2* promoter upstream of 1 kb (Supplementary Table S5).

In this study, we observed that the inhibitors of PI metabolism disturbs the early Al response events including nuclear localization of STOP1, and the expression of its target genes (Fig. 7). PI signaling is crucial as a second messenger in various events in plants such as development and stress responses (Xue *et al.*, 2009). Wu *et al.* (2019) first identified that the PI4K and PLC inhibitors (i.e. PAO and U73122) inhibit Al-induced expression of several genes including *AtALMT1*. Additionally, Al-induced *AtALMT1* expression was supressed by mutations in *PI4KIIIβ* (Wu *et al.*, 2019). Interestingly, *PI4KIIIβ1* and *PI4KIIIβ2* are involved in primary and lateral root growth/development (Rubilar-Hernández *et al.*, 2019), and are mainly localized in the Golgi apparatus (Simon *et al.*, 2014), where STOP1 proteins are located under control conditions (Supplementary Fig. S7). Future research is needed to clarify how and where STOP1 responds to PI signaling during Al exposure. In addition, PI signaling is also involved in other non-STOP1 Al-induced pathways, as transcription of Al-inducible genes which were not regulated by STOP1 were also supressed by the PI4K and PLC inhibitors (Wu *et al.*, 2019). Jones and Kochian (1995) reported that PLC activity in the roots was inhibited by Al, and $IP_3$ concentrations were altered when wheat roots were exposed to Al. A similar result was observed in cell cultures of coffee (Poot-Poot and Hernandez-Sotomayor, 2011). In addition, Al directly binds several plasma membrane lipids, and $PI(4,5)P_2$ has a very high binding affinity with $Al^{3+}$ (Jones and Kochian, 1997). Moreover, the STOP1/AtALMT1 system also plays a critical role in low P responses in plants (Balzergue *et al.*, 2017; Mora-Macías *et al.*, 2017). Several reports have shown that inositol phosphate (IP) kinases, such as IPK1 (inositol-pentaphosphate-2-kinase) regulate internal phosphate homeostasis by activating several phosphate starvation-induced genes including phosphate transporters in plants and yeasts (Norbis *et al.*, 1997; Schell *et al.*, 1999; Stevenson-Paulik *et al.*, 2005; Kuo *et al.*, 2014, 2018). IP metabolism is in the latter portion of the PI metabolic pathway, and is derived from $IP_3$ (Fig. 7A; Munnik and Nielsen, 2011). These observations suggest that phospholipid metabolism is a

bars correspond to an RAS>0.2. The positions in the native *AtALMT1* promoter sequence are indicated by letters in white font below the graph. (B) Comparison between the highlighted *AtALMT1* promoter CIS-D region, the identified STOP1-binding sites of *GDH2*-CIS1, *STOP2*-CIS1, and *AtMATE*-CIS2. Nucleotides in the STOP1-binding sites [corresponding to the letters in white font in panel (A)] are boxed, and different nucleotides in *GDH2*-CIS1, *STOP2*-CIS1 and *AtMATE*-CIS2 are shaded. (C) Comparison of STOP1 binding affinity of *AtMATE* -CIS2 with *AtALMT1* CIS-D, and *GDH2*-CIS1. The binding capacity was determined by AlphaScreen system. AlphaScreen signals were analysed in a competitive assay mixing reactive biotinylated *AtALMT1* CIS-D probe and non-biotinylated competitor probe at 1:1 or 1:10 molar ratio. Data are presented as the mean ±SD ($n$=3). Different letters indicate a significant difference ($P$<0.05, Tukey's test). AC, absence of competitor.

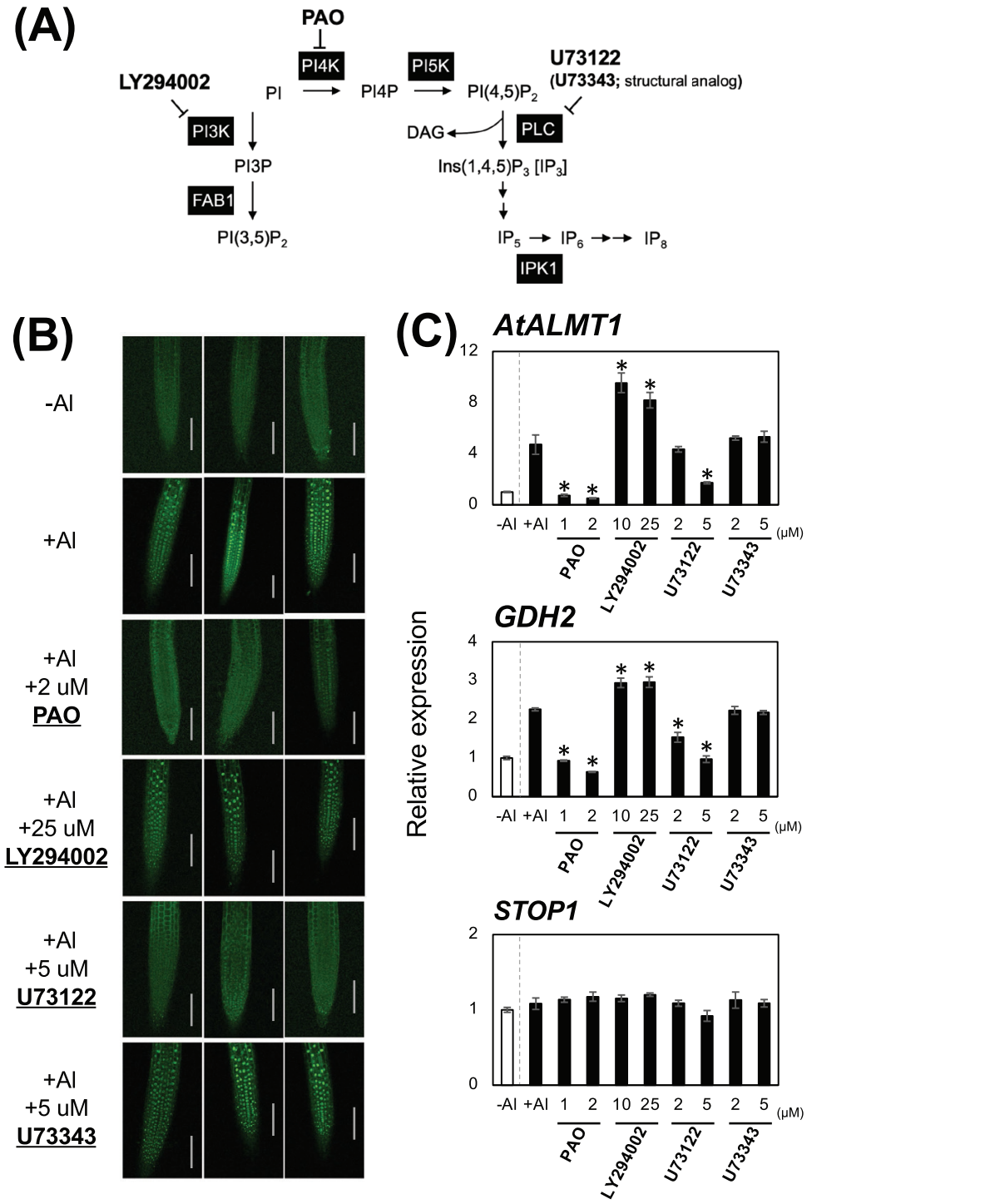


**Fig. 7.** Evaluation of several phosphoinositide (PI) metabolism inhibitors on the early Al-induced responses. (A) Schematic representation of PI and inositol phosphates (IP) metabolic pathways, and the inhibitors used in this study. PAO (phenylarsine oxide), FAB1 (fatty acid biosynthesis1), IPK1 (inositol-pentaphosphate-2-kinase), and DAG (diacylglycerol). (B) Evaluation of the several PI metabolism inhibitors effect on Al-induced STOP1 nuclear localization. The five day-old seedlings of transgenic plants carrying *STOP1* promoter*::STOP1-GFP* were treated with or without the inhibitor for 30 min as pre-treatment, and then incubated in the solution containing 10 μM $AlCl_3$(or no $AlCl_3$) with (or without) the corresponding inhibitor for 1.5 h. Fluorescence images of STOP1-GFP in the roots were observed by confocal microscopy, and three representative images are shown. Bar =100 μm. (C) Effect of the PI inhibitors on Al-induced transcription of *AtALMT1*, *GDH2*, and *STOP1*. The Col-0 seedings were pretreated with or without the inhibitors for 30 min before Al treatment. The seedlings were transferred to solution containing 10 μM $AlCl_3$ (or without $AlCl_3$) with or without the corresponding inhibitor, and incubated for 1.5 h. Expression was determined by quantitative real-time PCR using *UBQ1* as an internal control for expression, and the relative expression was calculated relative to expression in –Al. Data are presented as the mean ±SD ($n$=3). Asterisks indicate a significant difference from the expression in +Al without inhibitor (*$P$<0.05; Student's $t$-test).

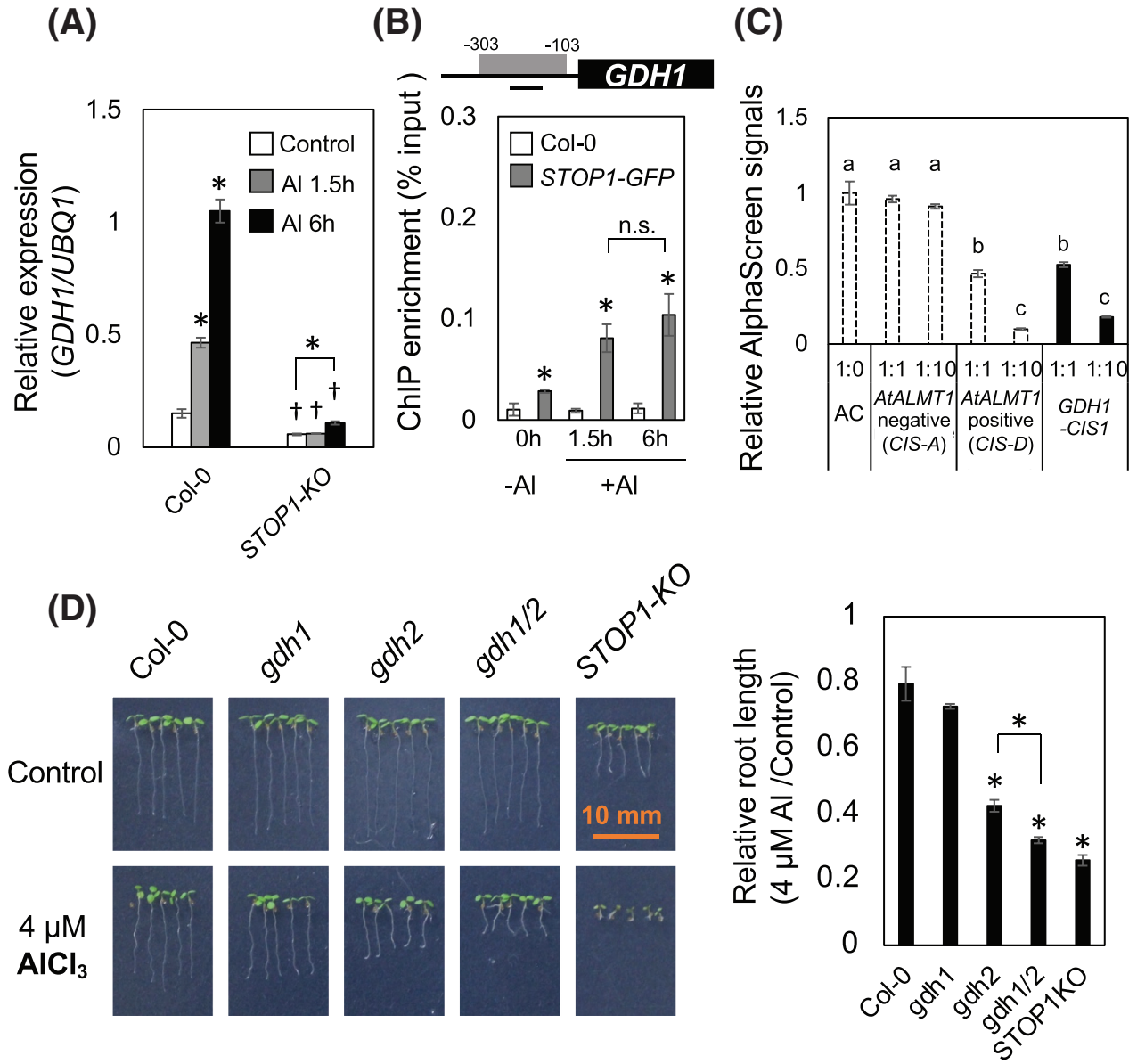


**Fig. 8.** Involvement of STOP1 on Al-induced *GDH1* expression and root growth in T-DNA insertion mutants for *gdh1, gdh2*, and *gdh1/2* in response to Al stress. (A) Expression of *GDH1* in Col-0 and *STOP1-KO* lines. The seedlings were treated with solution containing 10 μM $AlCl_3$ or without $AlCl_3$. The expression of *GDH1* was determined by quantitative real-time PCR and normalized against *UBQ1* expression. Data are presented as the mean ±SD (*n*=3). Asterisks and daggers indicate significant difference of expression from control condition, and Col-0, respectively (* or †*P*<0.05; Student's *t*-test). (B) Chromatin immunoprecipitation-quantitative PCR analysis for the *GDH1* promoter. Diagram above the graph shows the position of the potential STOP1 binding region that was identified by DAP-seq analysis (gray shaded box, DAP-seq peak data from O'Malley *et al.*, 2016), and the amplified region (black bar under DAP-seq peak) in the *GDH1* loci. Data are presented as the mean ±SD (*n*=3). Asterisks indicate a significant difference from Col-0 (**P*<0.05; Student's *t*-test). n.s., no significant difference. (C) Comparison of binding capacity of STOP1 to the *GDH1* and *AtALMT1* promoters. The *in vitro* STOP1 binding capacity was determined using the AlphaScreen system, and the signals were analysed in a competitive assay mixing reactive biotinylated *AtALMT1-D* probe and non-biotinylated competitor probe at 1:1 or 1:10 molar ratio. Data are presented as the relative AlphaScreen signal (absence of competitor (AC) was set as 1) ±SD (*n*=3). Different letters indicate a significant difference (*P*<0.05, Tukey's test). Relative AlphaScreen signals of AC, *AtALMT1*-negative, and *AtALMT1* positive (white bars) are also shown in Fig. 6C. (D) Root growth of T-DNA insertion mutants under Al-stress conditions. Seedlings of Col-0 (wild-type) and a series of T-DNA knockout (KO) mutants (*gdh1, gdh2, gdh1/2,* and *STOP1KO*) were grown for 5 d in 4 μM $AlCl_3$ or control (no $AlCl_3$) solutions (pH 5.0). Relative root lengths [RRL; toxic Al/control] ±SE are presented (*n*=5). Asterisks indicate significant difference from the RRL of the Col-0 plants, or between *gdh2* and *gdh1/2* (**P*<0.05; Student's *t*-test).

common target of Al toxicity and P deficiency, which may help explain the pleiotropic effects of STOP1/AtALMT1 in Al tolerance and P deficiency responses.

Regulation of the early Al response of *GDHs* by STOP1 caused another important pleiotropic role of STOP1 in stress tolerance. Previously, it was reported that *gdh1/gdh2*

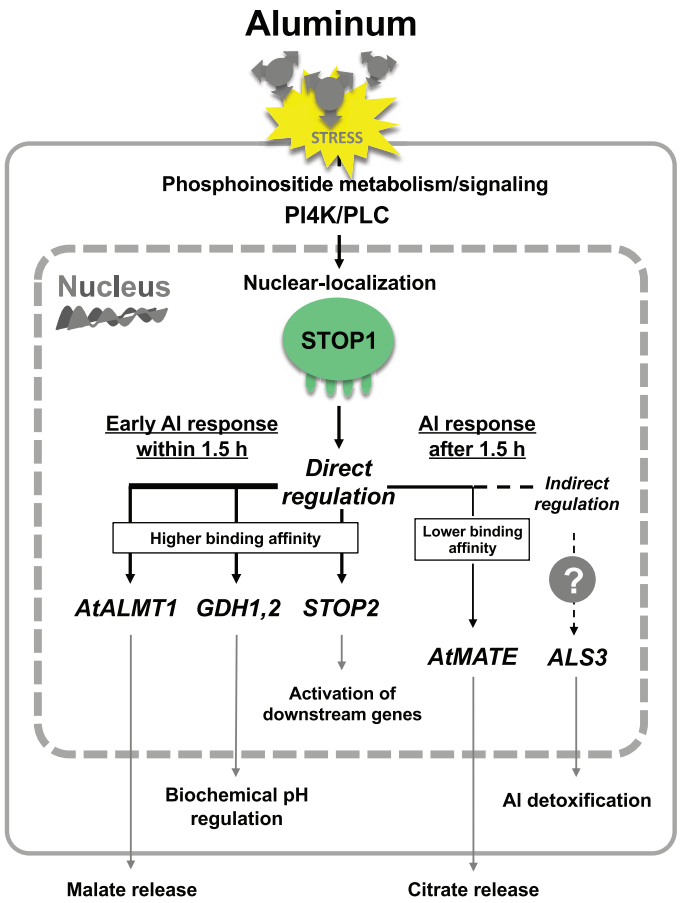


**Fig. 9.** Schematic representation of STOP1-mediated transcriptional regulation of its target genes under Al-stress conditions. Aluminum activates the transcription of the primary targets of STOP1, including *AtALMT1*, *GDH1, GDH2*, *STOP2*, and *AtMATE* which carry the STOP1-binding site in the promoter. In contrast, Al up-regulated expression of *ALS3*, whose promoter lacks a STOP1-binding site, is suggested to occur by an unidentified mechanism. The Al-induced expression of *AtMATE* and *ALS3* requires a longer Al exposure period than that of *AtALMT1*, *GDHs*, and *STOP2* (3 h, Fig. 4A). The slower Al response might be explained by weak binding of STOP1 to the promoter or indirect regulation of STOP1. The early Al-induced expression of STOP1-regulated genes (within 1.5 h) is associated with the localization of STOP1 to the nucleus, and this event is inhibited by PI4K and PLC inhibitors.

was sensitive to low pH and hypoxia/anoxia stress (Tsai *et al.*, 2016; Enomoto *et al.*, 2019). In this study, we found that the double *gdh1/gdh2* mutant also had highly suppressed Al tolerance (Fig. 8D). A link to Al and proton responses is reported by the work of Moseyko and Feldman (2001), who observed Al-induced cytosolic acidification using pH-sensitive GFP, while Ahn *et al.* (2001) reported that Al exposure inhibited the plasma membrane $H^+$-ATPase. Therefore, STOP1/GDHs may contribute to cellular pH homeostasis under Al stress in Arabidopsis. This hypothesis is supported by our root growth assays where the *gdh1/2* double mutant exhibited root growth inhibition at pH 5.0 with Al, but the inhibition was not observed without Al at the same pH (i.e. control conditions in Fig. 8D). It revealed that GDHs play crucial roles in stress tolerance as junction enzymes that connect carbon and nitrogen metabolism (Labboun *et al.*, 2009; Fontaine *et al.*, 2012), which are associated with pH-regulated metabolic pathways, namely the GABA shunt (Bown and Shelp, 2020) and other biochemical pathways (Sakano, 1998). Involvement of GDHs has been reported in other organisms adapted to low pH environments such as *Helicobacter pylori* (Miller and Maier, 2014) and fish adapted to acidic lakes (Hirata *et al.*, 2003). Andersson and Roger (2003) reported lateral gene transfer of GDHs within and between prokaryotes and eukaryotes. It suggests that GDHs are critical for protecting cells from cytosolic acidification in various organisms. *NtSTOP1*-RNAi suppressed proton and hypoxia tolerance of tobacco (Ito *et al.*, 2019; Enomoto *et al.*, 2019), suggesting that regulation of *GDH*s by STOP1-like proteins is conserved in various plants. Additionally, under Al stress, Al-induced GDHs may modulate low amounts of glutamate which inhibit root elongation by depolymerizing microtubules and depolarizing the plasma membrane (Sivaguru *et al.*, 2003).

In the present study, we found that accumulation of STOP1 in the nucleus almost immediately activates transcription of *AtALMT1* and *GDHs*, which encode proteins that have pleiotropic roles in stress tolerance. Previous studies identified that STOP1-regulating systems are conserved in a wide range of plant species (Ohyama *et al.*, 2013). In fact, NtSTOP1 in tobacco regulates common Al-tolerance genes such as *MATE* and *GDHs* (Ohyama *et al.*, 2013; Ito *et al.*, 2019). However, the pleiotropy of STOP1 appears to be variable across plant species. For example, *art1* (mutant of rice ortholog of STOP1) suppressed Al tolerance but not proton tolerance (Yamaji *et al.*, 2009), and VuSTOP1 in rice bean may regulate proton tolerance rather than Al tolerance (Fan *et al.*, 2015). These differences could be caused by the variation of the copy number of STOP1 and its regulated genes among different plant species. Further research is needed to identify the mechanisms underlying the variation related to the functioning of the STOP1 system in different plant species.

## Supplementary data

The following supplementary data are available at *JXB* online.

Fig. S1. Validation of stability of the expression of internal reference gene *UBQ1* for the expression analysis.

Fig. S2. Images of the fluorescence of GFP proteins in the roots of transgenic *Arabidopsis thaliana* plants carrying the *STOP1 promoter::GFP* after control or 10 μM $AlCl_3$ treatments.

Fig. S3. Promoter-scanning graphs presenting the over-represented octamer units in the promoters of STOP1-regulated genes.

Fig. S4. Competitive assays of *GDH2*-CIS1 and *STOP2*-CIS1 probes with or without the mutated CIS1 regions.

Fig. S5. Effect of phosphoinositide signaling inhibitors on Al-induced *STOP2* expression.

Fig. S6. Identification of the STOP1 binding sequence in the *GDH1* promoter.

Fig. S7. Localization of STOP1-GFP in the Golgi apparatus under control conditions.

Fig. S8. Homology-based 3D model of the STOP1-*ALMT1* (CIS-D) transcriptional module.

Fig. S9. A genome browser view of bisulfite-seq of Col-0 root tips in the *AtMATE* loci.

Table S1. Details regarding the PCR primers.

Table S2. Genes whose expression was suppressed by the *stop1* mutation under Al stress conditions.

Table S3. Over-represented octamer units in the promoter of genes whose Al-induced expression was suppressed by the *stop1* mutation.

Table S4. Sequence and position of probes used in the *in vitro* assay assessing the binding of dsDNA and STOP1.

Table S5. The WRKY- or CAMATA-binding motifs in *GDH1* and *GDH2* promoters.

Video S1. Time-lapse images of the localization of STOP1-GFP in the nucleus during a 1.5 h Al treatment.

## Acknowledgements

We thank Mr Katsuki Fujii for his technical assistance during the analysis of the *ALS3* promoter, and Dr Naoki Takahashi (Nara institute of science and technology, Japan) for providing the protocol of ChIP analysis. The series of *gdh* mutants was kindly provided by Dr Allen G. Good (University of Alberta, Canada). This work was supported by a grant from the Japan Society for the Promotion of Science Project Nos: 15H04468, 15KT0029, and 18H02113 to HK as well as KAKENHI and 13J08738 to MT), and a Canada Excellence Research Chairs grant and Global Institute for Food Security funding to LVK.

## Author contributions

MT and HK conceived and designed the project; LVK and HK supervised research; MT, TE, and HI performed the experiments; LW, YK, SI, MK, MN, YT, MF, KS, and YYY provided technical assistance of the experiments and analyses; JM, and DA conducted *in silico* homology-based 3D modeling analysis; MT, JM, LVK, and HK analysed data and wrote the article.

## Conflict of interest

The authors declare no conflict of interest.

## Data availability

All data supporting the findings of this study are available within the paper and within its supplementary data published online.

## References

**Ahn SJ, Sivaguru M, Osawa H, Chung GC, Matsumoto H.** 2001. Aluminum inhibits the H(+)-ATPase activity by permanently altering the plasma membrane surface potentials in squash roots. Plant Physiology **126**, 1381–1390.

**Andersson JO, Roger AJ.** 2003. Evolution of glutamate dehydrogenase genes: evidence for lateral gene transfer within and between prokaryotes and eukaryotes. BMC Evolutionary Biology **3**, 14.

**Balzergue C, Dartevelle T, Godon C, *et al.*** 2017. Low phosphate activates STOP1-ALMT1 to rapidly inhibit root cell elongation. Nature Communications **8**, 15300.

**Barros VA, Chandnani R, de Sousa SM, Maciel LS, Tokizawa M, Guimaraes CT, Magalhaes JV, Kochian LV.** 2020. Root adaptation via common genetic factors conditioning tolerance to multiple stresses for crops cultivated on acidic tropical soils. Frontiers in Plant Science **11**, 565339.

**Bown AW, Shelp BJ.** 2020. Does the GABA shunt regulate cytosolic GABA? Trends in Plant Science **25**, 422–424.

**Dietrich K, Weltmeier F, Ehlert A, Weiste C, Stahl M, Harter K, Dröge-Laser W.** 2011. Heterodimers of the Arabidopsis transcription factors bZIP1 and bZIP53 reprogram amino acid metabolism during low energy stress. The Plant Cell **23**, 381–395.

**Ding ZJ, Yan JY, Xu XY, Li GX, Zheng SJ.** 2013. WRKY46 functions as a transcriptional repressor of *ALMT1*, regulating aluminum-induced malate secretion in *Arabidopsis*. Plant Journal **76**, 825–835.

**Enomoto T, Tokizawa M, Ito H, Iuchi S, Kobayashi M, Yamamoto YY, Kobayashi Y, Koyama H.** 2019. STOP1 regulates the expression of HsfA2 and GDHs that are critical for low-oxygen tolerance in Arabidopsis. Journal of Experimental Botany **70**, 3297–3311.

**Eulgem T, Rushton PJ, Robatzek S, Somssich IE.** 2000. The WRKY superfamily of plant transcription factors. Trends in Plant Science **5**, 199–206.

**Fan W, Lou HQ, Gong YL, Liu MY, Cao MJ, Liu Y, Yang JL, Zheng SJ.** 2015. Characterization of an inducible C2 H2 -type zinc finger transcription factor VuSTOP1 in rice bean (*Vigna umbellata*) reveals differential regulation between low pH and aluminum tolerance mechanisms. New Phytologist **208**, 456–468.

**Fang Q, Zhang J, Zhang Y, Fan N, van den Burg HA, Huang CF.** 2020. Regulation of aluminum resistance in Arabidopsis involves the SUMOylation of the zinc finger transcription factor STOP1. The Plant Cell **32**, 3921–3938.

**Fontaine JX, Terce-Laforgue T, Armengaud P, *et al.*** 2012. Characterization of a NADH-dependent glutamate dehydrogenase mutant of Arabidopsis demonstrates the key role of this enzyme in root carbon and nitrogen metabolism. Plant Cell **24**, 4044–4065.

**Foster R, Izawa T, Chua NH.** 1994. Plant bZIP proteins gather at ACGT elements. FASEB Journal **8**, 192–200.

**Fujimoto M, Suda Y, Vernhettes S, Nakano A, Ueda T.** 2015. Phosphatidylinositol 3-kinase and 4-kinase have distinct roles in intracellular trafficking of cellulose synthase complexes in *Arabidopsis thaliana*. Plant & Cell Physiology **56**, 287–298.

**Fujiwara T, Hirai MY, Chino M, Komeda Y, Naito S.** 1992. Effects of sulfur nutrition on expression of the soybean seed storage protein genes in transgenic petunia. Plant Physiology **99**, 263–268.

**Gabrielson KM, Cancel JD, Morua LF, Larsen PB.** 2006. Identification of dominant mutations that confer increased aluminium tolerance through mutagenesis of the Al-sensitive Arabidopsis mutant, *als3-1*. Journal of Experimental Botany **57**, 943–951.

**Gendrel AV, Lippman Z, Martienssen R, Colot V.** 2005. Profiling histone modification patterns in plants using genomic tiling microarrays. Nature Methods **2**, 213–218.

**Godon C, Mercier C, Wang X, David P, Richaud P, Nussaume L, Liu D, Desnos T.** 2019. Under phosphate starvation conditions, Fe and Al trigger accumulation of the transcription factor STOP1 in the nucleus of Arabidopsis root cells. Plant Journal **99**, 937–949.

**Guo J, Zhang Y, Gao H, Li S, Wang ZY, Huang CF.** 2020. Mutation of HPR1 encoding a component of the THO/TREX complex reduces STOP1

accumulation and aluminium resistance in *Arabidopsis thaliana*. New Phytologist **228**, 179–193.

**Higo K, Ugawa Y, Iwamoto M, Korenaga T.** 1999. Plant cis-acting regulatory DNA elements (PLACE) database: 1999. Nucleic Acids Research **27**, 297–300.

**Hirata T, Kaneko T, Ono T, *et al.*** 2003. Mechanism of acid adaptation of a fish living in a pH 3.5 lake. American Journal of Physiology. Regulatory, Integrative and Comparative Physiology **284**, R1199–R1212.

**Hoekenga OA, Maron LG, Pineros MA, *et al.*** 2006. *AtALMT1*, which encodes a malate transporter, is identified as one of several genes critical for aluminum tolerance in *Arabidopsis*. Proceedings of the National Academy of Sciences, USA **103**, 9738–9743.

**Hruz T, Laule O, Szabo G, Wessendorp F, Bleuler S, Oertle L, Widmayer P, Gruissem W, Zimmermann P.** 2008. Genevestigator v3: a reference expression database for the meta-analysis of transcriptomes. Advances in Bioinformatics **2008**, 420747.

**Ito H, Kobayashi Y, Yamamoto YY, Koyama H.** 2019. Characterization of NtSTOP1-regulating genes in tobacco under aluminum stress. Soil Science and Plant Nutrition **65**, 251–258.

**Iuchi S, Koyama H, Iuchi A, Kobayashi Y, Kitabayashi S, Kobayashi Y, Ikka T, Hirayama T, Shinozaki K, Kobayashi M.** 2007. Zinc finger protein STOP1 is critical for proton tolerance in Arabidopsis and coregulates a key gene in aluminum tolerance. Proceedings of the National Academy of Sciences, USA **104**, 9900–9905.

**Jones DL, Kochian LV.** 1995. Aluminum inhibition of the inositol 1,4,5-trisphosphate signal transduction pathway in wheat roots: a role in aluminum toxicity? The Plant Cell **7**, 1913–1922.

**Jones DL, Kochian LV.** 1997. Aluminum interaction with plasma membrane lipids and enzyme metal binding sites and its potential role in Al cytotoxicity. FEBS Letters **400**, 51–57.

**Kang SG, Price J, Lin PC, Hong JC, Jang JC.** 2010. The Arabidopsis bZIP1 transcription factor is involved in sugar signaling, protein networking, and DNA binding. Molecular Plant **3**, 361–373.

**Kawakatsu T, Stuart T, Valdes M, *et al.*** 2016. Unique cell-type-specific patterns of DNA methylation in the root meristem. Nature Plants **2**, 16058.

**Kobayashi Y, Hoekenga OA, Itoh H, Nakashima M, Saito S, Shaff JE, Maron LG, Piñeros MA, Kochian LV, Koyama H.** 2007. Characterization of *AtALMT1* expression in aluminum-inducible malate release and its role for rhizotoxic stress tolerance in *Arabidopsis*. Plant Physiology **145**, 843–852.

**Kobayashi Y, Kobayashi Y, Sugimoto M, Lakshmanan V, Iuchi S, Kobayashi M, Bais HP, Koyama H.** 2013a. Characterization of the complex regulation of *AtALMT1* expression in response to phytohormones and other inducers. Plant Physiology **162**, 732–740.

**Kobayashi Y, Lakshmanan V, Kobayashi Y, Asai M, Iuchi S, Kobayashi M, Bais HP, Koyama H.** 2013b. Overexpression of *AtALMT1* in the *Arabidopsis thaliana* ecotype Columbia results in enhanced Al-activated malate excretion and beneficial bacterium recruitment. Plant Signaling & Behavior **8**, e25565

**Kobayashi Y, Ohyama Y, Kobayashi Y, *et al.*** 2014. STOP2 activates transcription of several genes for Al- and low pH-tolerance that are regulated by STOP1 in *Arabidopsis*. Molecular Plant **7**, 311–322.

**Kochian LV, Hoekenga OA, Pineros MA.** 2004. How do crop plants tolerate acid soils? Mechanisms of aluminum tolerance and phosphorous efficiency. Annual Review of Plant Biology **55**, 459–493.

**Kochian LV, Piñeros MA, Liu J, Magalhaes JV.** 2015. Plant adaptation to acid soils: the molecular basis for crop aluminum resistance. Annual Review of Plant Biology **66**, 571–598.

**Kopittke PM, Moore KL, Lombi E, *et al.*** 2015. Identification of the primary lesion of toxic aluminum in plant roots. Plant Physiology **167**, 1402–1411.

**Krieger E, Vriend G.** 2014. YASARA View - molecular graphics for all devices - from smartphones to workstations. Bioinformatics **30**, 2981–2982.

**Krtková J, Havelková L, Křepelová A, Fišer R, Vosolsobě S, Novotná Z, Martinec J, Schwarzerová K.** 2012. Loss of membrane fluidity and endocytosis inhibition are involved in rapid aluminum-induced root growth cessation in *Arabidopsis thaliana*. Plant Physiology and Biochemistry **60**, 88–97.

**Kuo HF, Chang TY, Chiang SF, Wang WD, Charng YY, Chiou TJ.** 2014. Arabidopsis inositol pentakisphosphate 2-kinase, AtIPK1, is required for growth and modulates phosphate homeostasis at the transcriptional level. Plant Journal **80**, 503–515.

**Kuo HF, Hsu YY, Lin WC, Chen KY, Munnik T, Brearley CA, Chiou TJ.** 2018. Arabidopsis inositol phosphate kinases IPK1 and ITPK1 constitute a metabolic pathway in maintaining phosphate homeostasis. Plant Journal **95**, 613–630.

**Labboun S, Tercé-Laforgue T, Roscher A, *et al.*** 2009. Resolving the role of plant glutamate dehydrogenase. I. In vivo real time nuclear magnetic resonance spectroscopy experiments. Plant & Cell Physiology **50**, 1761–1773.

**Lakshmanan V, Kitto SL, Caplan JL, Hsueh YH, Kearns DB, Wu YS, Bais HP.** 2012. Microbe-associated molecular patterns-triggered root responses mediate beneficial rhizobacterial recruitment in *Arabidopsis*. Plant Physiology **160**, 1642–1661.

**Larsen PB, Geisler MJ, Jones CA, Williams KM, Cancel JD.** 2005. ALS3 encodes a phloem-localized ABC transporter-like protein that is required for aluminum tolerance in Arabidopsis. Plant Journal **41**, 353–363.

**Liu J, Magalhaes JV, Shaff J, Kochian LV.** 2009. Aluminum-activated citrate and malate transporters from the MATE and ALMT families function independently to confer *Arabidopsis* aluminum tolerance. Plant Journal **57**, 389–399.

**Martinez A, Traverso JA, Valot B, Ferro M, Espagne C, Ephritikhine G, Zivy M, Giglione C, Meinnel T.** 2008. Extent of N-terminal modifications in cytosolic proteins from eukaryotes. Proteomics **8**, 2809–2831.

**Miller EF, Maier RJ.** 2014. Ammonium metabolism enzymes aid *Helicobacter pylori* acid resistance. Journal of Bacteriology **196**, 3074–3081.

**Mitsuhara I, Ugaki M, Hirochika H, *et al*.** 1996. Efficient promoter cassettes for enhanced expression of foreign genes in dicotyledonous and monocotyledonous plants. Plant & Cell Physiology **37**, 49–59.

**Miyashita Y, Good AG.** 2008. NAD(H)-dependent glutamate dehydrogenase is essential for the survival of *Arabidopsis thaliana* during dark-induced carbon starvation. Journal of Experimental Botany **59**, 667–680.

**Mora-Macías J, Ojeda-Rivera JO, Gutiérrez-Alanís D, Yong-Villalobos L, Oropeza-Aburto A, Raya-González J, Jiménez-Domínguez G, Chávez-Calvillo G, Rellán-Álvarez R, Herrera-Estrella L.** 2017. Malate-dependent Fe accumulation is a critical checkpoint in the root developmental response to low phosphate. Proceedings of the National Academy of Sciences, USA **114**, E3563–E3572.

**Moseyko N, Feldman LJ.** 2001. Expression of pH-sensitive green fluorescent protein in *Arabidopsis thaliana*. Plant, Cell & Environment **24**, 557–563.

**Munnik T, Nielsen E.** 2011. Green light for polyphosphoinositide signals in plants. Current Opinion in Plant Biology **14**, 489–497.

**Nomoto M, Tada Y.** 2018. Cloning-free template DNA preparation for cell-free protein synthesis via two-step PCR using versatile primer designs with short 3'-UTR. Genes to Cells **23**, 46–53.

**Norbis F, Boll M, Stange G, Markovich D, Verrey F, Biber J, Murer H.** 1997. Identification of a cDNA/protein leading to an increased Pi-uptake in *Xenopus laevis* oocytes. The Journal of Membrane Biology **156**, 19–24.

**Ogita N, Okushima Y, Tokizawa M, *et al.*** 2018. Identifying the target genes of SUPPRESSOR OF GAMMA RESPONSE 1, a master transcription factor controlling DNA damage response in Arabidopsis. Plant Journal **94**, 439–453.

**Ohyama Y, Ito H, Kobayashi Y, *et al.*** 2013. Characterization of AtSTOP1 orthologous genes in tobacco and other plant species. Plant Physiology **162**, 1937–1946.

**O'Malley RC, Huang SC, Song L, Lewsey MG, Bartlett A, Nery JR, Galli M, Gallavotti A, Ecker JR.** 2016. Cistrome and epicistrome features shape the regulatory DNA landscape. Cell **165**, 1280–1292.

**Para A, Li Y, Marshall-Colon A, *et al.*** 2014. Hit-and-run transcriptional control by bZIP1 mediates rapid nutrient signaling in *Arabidopsis*. Proceedings of the National Academy of Sciences, USA **111**, 10371–10376.

**Parre E, Ghars MA, Leprince AS, Thiery L, Lefebvre D, Bordenave M, Richard L, Mazars C, Abdelly C, Savouré A.** 2007. Calcium signaling via phospholipase C is essential for proline accumulation upon ionic but

not nonionic hyperosmotic stresses in Arabidopsis. Plant Physiology **144**, 503–512.

**Patel A, Yang P, Tinkham M, *et al.*** 2018. DNA conformation induces adaptable binding by tandem zinc finger proteins. Cell **173**, 221–233.e12.

**Poot-Poot W, Hernandez-Sotomayor SM.** 2011. Aluminum stress and its role in the phospholipid signaling pathway in plants and possible biotechnological applications. IUBMB Life **63**, 864–872.

**Riveras E, Alvarez JM, Vidal EA, Oses C, Vega A, Gutiérrez RA.** 2015. The calcium ion is a second messenger in the nitrate signaling pathway of Arabidopsis. Plant Physiology **169**, 1397–1404.

**Rubilar-Hernández C, Osorio-Navarro C, Cabello F, Norambuena L.** 2019. PI4KIIIβ activity regulates lateral root formation driven by endocytic trafficking to the vacuole. Plant Physiology **181**, 112–126.

**Rudrappa T, Czymmek KJ, Paré PW, Bais HP.** 2008. Root-secreted malic acid recruits beneficial soil bacteria. Plant Physiology **148**, 1547–1556.

**Sakano K.** 1998. Revision of biochemical pH-Stat: involvement of alternative pathway metabolisms. Plant & Cell Physiology **39**, 467–473.

**Sasaki T, Yamamoto Y, Ezaki B, Katsuhara M, Ahn SJ, Ryan PR, Delhaize E, Matsumoto H.** 2004. A wheat gene encoding an aluminum-activated malate transporter. Plant Journal **37**, 645–653.

**Sauret-Güeto S, Schiessl K, Bangham A, Sablowski R, Coen E.** 2013. JAGGED controls *Arabidopsis* petal growth and shape by interacting with a divergent polarity field. PLoS Biology **11**, e1001550.

**Sawaki Y, Iuchi S, Kobayashi Y, *et al.*** 2009. STOP1 regulates multiple genes that protect *Arabidopsis* from proton and aluminum toxicities. Plant Physiology **150**, 281–294.

**Schell MJ, Letcher AJ, Brearley CA, Biber J, Murer H, Irvine RF.** 1999. PiUS (Pi uptake stimulator) is an inositol hexakisphosphate kinase. FEBS Letters **461**, 169–172.

**Simon ML, Platre MP, Assil S, van Wijk R, Chen WY, Chory J, Dreux M, Munnik T, Jaillais Y.** 2014. A multi-colour/multi-affinity marker set to visualize phosphoinositide dynamics in Arabidopsis. Plant Journal **77**, 322–337.

**Sivaguru M, Pike S, Gassmann W, Baskin TI.** 2003. Aluminum rapidly depolymerizes cortical microtubules and depolarizes the plasma membrane: evidence that these responses are mediated by a glutamate receptor. Plant & Cell Physiology **44**, 667–675.

**Stevenson-Paulik J, Bastidas RJ, Chiou ST, Frye RA, York JD.** 2005. Generation of phytate-free seeds in Arabidopsis through disruption of inositol polyphosphate kinases. Proceedings of the National Academy of Sciences, USA **102**, 12612–12617.

**Sun C, Palmqvist S, Olsson H, Borén M, Ahlandsberg S, Jansson C.** 2003. A novel WRKY transcription factor, SUSIBA2, participates in sugar signaling in barley by binding to the sugar-responsive elements of the iso1 promoter. The Plant Cell **15**, 2076–2092.

**Takahashi S, Monda K, Higaki T, Hashimoto-Sugimoto M, Negi J, Hasezawa S, Iba K.** 2017. Differential effects of phosphatidylinositol 4-kinase (PI4K) and 3-kinase (PI3K) inhibitors on stomatal responses to environmental signals. Frontiers in Plant Science **8**, 677.

**Tokizawa M, Kobayashi Y, Saito T, Kobayashi M, Iuchi S, Nomoto M, Tada Y, Yamamoto YY, Koyama H.** 2015. SENSITIVE TO PROTON RHIZOTOXICITY1, CALMODULIN BINDING TRANSCRIPTION ACTIVATOR2, and other transcription factors are involved in ALUMINUM-ACTIVATED MALATE TRANSPORTER1 expression. Plant Physiology **167**, 991–1003.

**Tokizawa M, Kusunoki K, Koyama H, Kurotani A, Sakurai T, Suzuki Y, Sakamoto T, Kurata T, Yamamoto YY.** 2017. Identification of Arabidopsis genic and non-genic promoters by paired-end sequencing of TSS tags. Plant Journal **90**, 587–605.

**Tsai KJ, Lin CY, Ting CY, Shih MC.** 2016. Ethylene-regulated glutamate dehydrogenase fine-tunes metabolism during anoxia-reoxygenation. Plant Physiology **172**, 1548–1562.

**Tsutsui T, Yamaji N, Feng Ma J.** 2011. Identification of a *cis*-acting element of ART1, a C2H2-type zinc-finger transcription factor for aluminum tolerance in rice. Plant Physiology **156**, 925–931.

**von Uexküll HR, Mutert E.** 1995. Global extent, development and economic impact of acid soils. Plant and Soil **171**, 1–15.

**Wu L, Sadhukhan A, Kobayashi Y, *et al.*** 2019. Involvement of phosphatidylinositol metabolism in aluminum-induced malate secretion in Arabidopsis. Journal of Experimental Botany **70**, 3329–3342.

**Xue HW, Chen X, Mei Y.** 2009. Function and regulation of phospholipid signalling in plants. The Biochemical Journal **421**, 145–156.

**Yamaji N, Huang CF, Nagao S, Yano M, Sato Y, Nagamura Y, Ma JF.** 2009. A zinc finger transcription factor ART1 regulates multiple genes implicated in aluminum tolerance in rice. The Plant Cell **21**, 3339–3349.

**Yamamoto YY, Yoshioka Y, Hyakumachi M, Maruyama K, Yamaguchi-Shinozaki K, Tokizawa M, Koyama H.** 2011. Prediction of transcriptional regulatory elements for plant hormone responses based on microarray data. BMC Plant Biology **11**, 39.

**Yang T, Poovaiah BW.** 2002. A calmodulin-binding/CGCG box DNA-binding protein family involved in multiple signaling pathways in plants. The Journal of Biological Chemistry **277**, 45049–45058.

**Zhang Y, Zhang J, Guo J, Zhou F, Singh S, Xu X, Xie Q, Yang Z, Huang CF.** 2019. F-box protein RAE1 regulates the stability of the aluminum-resistance transcription factor STOP1 in Arabidopsis. Proceedings of the National Academy of Sciences, USA **116**, 319–327.